PHILOSOPHICAL TRANSACTIONS OF THE ROYAL SOCIETY A MATHEMATICAL, PHYSICAL & ENGINEERING SCIENCES

Fluid Transport in Lineaments

R. Kerrich

Phil. Trans. R. Soc. Lond. A 1986 **317**, 219-251
doi: 10.1098/rsta.1986.0033

Phil. Trans. R. Soc. Lond. A **317**, 219–251 (1986)

Printed in Great Britain

Fluid transport in lineaments

By R. Kerrich

Department of Geology, University of Western Ontario, London, Ontario, Canada N6A 5B7

Fluid infiltration into fault zones and their deeper level counterparts, brittle–ductile shear zones, is examined in five different tectonic environments. In the 2.7 Ga Abitibi Greenstone Belt major tectonic discontinuities have lateral extents of hundreds of kilometres. These structures, initiated as listric normal faults accommodating rift extension of the greenstone belt, acted as sites for the extrusion of komatiitic magmas, and formed submarine scarps which delimit linear belts of clastic and chemical sediments. During reverse motion on the structures, accommodating shortening of the belt, these transcrustal faults were used as a conduit for the ascent of trondhjemitic magmas from the base of the crust, alkaline magmas from the asthenosphere, and for discharge of hundreds of cubic kilometres of hydrothermal fluids. Such fluids were characterized by $\delta^{18}O = 6 \pm 2$, $\delta D = -50 \pm 20$, $\delta^{13}C = -4 \pm 3$, and temperatures of 270–450 °C, probably derived from devolatilization of crustal rocks undergoing prograde metamorphism. Hydrothermal fluids were more radiogenic ($^{87}Sr/^{86}Sr = 0.7010$–0.7040) and possessed higher values of μ than contemporaneous mantle, komatiites or tholeiites, and thus carried a contribution from older sialic basement. Mineralized faults possess enrichments of l.i.l. elements, including K, Rb, Li, Cs, B and CO_2, as well as rare elements such as Au, Ag, As, Sb, Se, Te, Bi, W. Fluids were characterized by $X_{CO_2} \approx 0.1$, neutral to slightly acidic pH, low salinity (less than 3% by mass), and $K/Na \approx 0.1$, carried minor CH_4, CO and N_2, and underwent transient effervescence of CO_2 during decompression.

At Yellowknife, a series of large-scale shear zones developed by brittle–ductile mechanisms, involving volume dilation with the migration of *ca.* 5% (by mass) volatiles into the shear zone from surrounding metabasalts. This early deformation involved no departures in redox state or whole-rock $\delta^{18}O$ from background states of $Fe^{2+}/\epsilon Fe = 0.7$ and $\delta^{18}O$ of 7–7.5‰ respectively, attesting to conditions of low water/rock ratios. Shear zones subsequently acted as high-permeability conduits for pulsed discharge of more than 9 km^3 of reduced metamorphic hydrothermal fluids at 360–450 °C. The West Bay Fault, a late major transcurrent structure, contains massive vein quartz that grew at 200–300 °C from fluids of 2–6% salinity (possibly formation brines).

At the Grenville Front, translation was accommodated along two mylonite zones and an intervening boundary fault. The high-temperature (MZ II) and low-temperature (MZ I) mylonite zones formed at 580–640 °C and 430–490 °C, respectively, in the presence of fluids of metamorphic origin, indigenous to the immediate rocks. A population of post-tectonic quartz veins occupying brittle fractures were precipitated from fluids with extremely negative $\delta^{18}O$ at 200–300 °C. The water may have been derived from downward penetration into fault zones of low ^{18}O precipitation on a mountain range induced by continental collision, with uplift accommodated at deep levels by the mylonite zones coupled with rebound on the boundary faults.

At Lagoa Real, Brazil, Archaean gneisses overlie Proterozoic sediments along thrust surfaces, and contain brittle–ductile shear zones locally occupied by uranium deposits. Following deformation at 500–540 °C, in the presence of metamorphic fluids and under conditions of low water/rock ratios, shear zones underwent local intense oxidation and desilication. All minerals undergo a shift of −10‰ $\delta^{18}O$, indicating discharge up through the Archaean gneisses of formation brines recharged by

meteoric water in the underlying Proterozoic sediments during overthrusting: about 1000 km^3 of solution passed through these structures. The shear zones and Proterozoic sediments are less radiogenic ($^{87}Sr/^{86}Sr = 0.720$) than contemporaneous Archaean gneisses ($^{87}Sr/^{86}Sr = 0.900$), corroborating transport of fluids and solutes through the structure from a large external reservoir.

Major crustal detachment faults of Tertiary age in the Picacho Cordilleran metamorphic core complex of Arizona show an upward transition from undeformed granitic basement, through mylonitic to brecciated and hydrothermally altered counterparts. The highest tectonic levels are allochthonous, oxidatively altered Miocene volcanics, with hydrothermal sediments in listric normal fault basins. This transition is accompanied by a 12‰ increase in $\delta^{18}O$ from 7 to 19, and a decrease of temperature of 400 °C, because of expulsion of large volumes of metamorphic fluids during detachment. In the Miocene allochthon, mixing occurred between cool downward-penetrating meteoric thermal waters and hot, deeper aqueous reservoirs.

In general, flow régimes in these fault and shear zones follow a sequence from conditions of high temperature and pressure with locally derived fluids at low water/rock ratios during initiation of the structures, to high fluxes of reduced formation or metamorphic fluids along conduits as the structures propagate and intersect hydrothermal reservoirs. Later in the tectonic evolution and at shallower crustal levels, there was incursion of oxidizing fluids from near-surface reservoirs into the faults.

1. Introduction

Fluid penetration through major structural lineaments, specifically faults and their deeper level extensions, brittle-ductile shear zones, is a well established phenomenon, both from contemporary observations of seismic pumping, and from hydration or extensive hydrothermal mineralization in ancient structural equivalents. Seismic pumping is the transient surface effusion of thermal waters along fault zones after moderate to large earthquakes in consolidated rocks (Sibson 1981*a*, *b*, 1982; Sibson *et al.* 1975).

The mechanical and chemical role of fluids in fault and shear zones has been examined by a number of authors for ancient structures (Beach & Fyfe 1972; Beach 1976; Kerrich *et al.* 1977*a*, 1980, 1984; Fyfe *et al.* 1978; Fyfe & Kerrich 1983, 1985) as well as their seismically active modern counterparts (Irwin & Barnes 1975; Sibson 1982 and this symposium). However, there is little quantitative information on the origin of fluid reservoirs implicated, the ambient temperature and pressure, physical and chemical properties, hydraulic conditions, or of the possible evolution of fluid régimes through a history of progressive incremental displacement along the structures.

This paper examines the variety of fluid régimes in lineaments with the use of information from structures in five areas that encompass a variety of tectonic environments, styles of deformation, lithological groups and ages. These are:

(i) fault systems of the Abitibi Greenstone Belt (*ca.* 2700 Ma);
(ii) brittle–ductile shear zones in the Yellowknife Greenstone Belt (*ca.* 2700 Ma);
(iii) structures at the Grenville Front (*ca.* 1100 Ma);
(iv) shear zones aged 820 Ma in Archaean gneisses at Lagoa Real, Brazil;
(v) detachment faults in Cordilleran metamorphic core complexes, of Tertiary age.

Selection of these structural domains was based on existing mapping and documentation of the faults as major structural features tens to hundreds of kilometres in lateral extent. In addition, the presence of sporadically developed mineralization provides the opportunity to evaluate fluid régimes associated with the faults.

PHILOSOPHICAL TRANSACTIONS OF THE ROYAL SOCIETY A MATHEMATICAL, PHYSICAL & ENGINEERING SCIENCES

Specific questions to be considered in the context of fluid transport through lineaments are:

(i) sources of volatile components such as H_2O, CO_2, H_2S;

(ii) the nature of rock reservoirs donating lithophile and other elements locally enriched in faults;

(iii) ambient temperature–pressure and hydraulic conditions;

(iv) the history of incremental displacement and fluid activity;

(v) the presence of highly sodic or alkaline magmas along some structural lineaments.

This paper draws on an earlier article concerning fluid participation in deep fault zones (Kerrich *et al.* 1984), reports new data for previously described regions, and extends coverage of the subject with reference to additional tectonic situations.

2. Abitibi greenstone belt faults

(*a*) *Geological setting*

The 2.7 Ga Abitibi Greenstone Belt, located in the Superior Province, is composed of an array of volcanic–plutonic complexes, with intervening belts of volcaniclastic, clastic and chemical sedimentary rocks (Goodwin & Ridler 1970). Prehnite–pumpellyite to lower greenschist facies of regional or hydrothermal metamorphism predominate, except in the periphery of batholiths where amphibolite facies rocks may be present (Jolly 1978).

A prominent feature of the greenstone belt is a series of major east–west trending tectonic discontinuities or fault zones, locally termed 'breaks', which extend for hundreds of kilometres (figure 1*a*, *b*). These structures control the linear disposition of ultramafic rocks, and locally delimit linear belts of clastic or chemical sedimentary rocks. The structures also acted as preferential sites for the emplacement of trondhjemitic and alkaline magmas, as well as being domains of intense hydrothermal metasomatism, exemplified by rich lode gold deposits.

(*b*) *Source of volatile components in fault zones*

The source, temperature and magnitude of aqueous fluid reservoirs participating in fault zones has been evaluated from oxygen and hydrogen isotope data. Five distinct terrestrial fluid reservoirs have been identified from their oxygen and hydrogen isotope compositional ranges. These are marine, meteoric, magmatic and metamorphic fluids, together with formation brines that generally contain a large component of 'evolved' meteoric recharge waters (Taylor 1974; figure 2*a*). Oxygen isotope studies also permit estimates of ambient mineral and fluid temperatures of equilibrium, given that the fractionation of oxygen isotopes between co-existing silicates or metal oxides is a function of temperature alone (Javoy 1977; Friedman & O'Neil 1977). Problems of identifying fluid flow through rocks are particularly amenable to evaluation by oxygen isotope analyses, because isotopic exchange between rocks and an aqueous reservoir is reflected in shifts of $\delta^{18}O$ (rock or mineral) from an initial value, by a magnitude that depends on the $\delta^{18}O$ of the fluid, the ambient temperature, and the fluid/rock ratio (Taylor 1974, 1979).

A compilation of oxygen isotope data for hydrothermal silicates from mineralized fault zones is given in Kerrich (1983), and calculated fluid isotopic compositions are summarized in figure 2*a*, incorporating new data. A significant feature of the mineral results is that the $\delta^{18}O$ values of hydrothermal quartz, muscovite and chlorite lie within narrow intervals, signifying uniform hydrothermal conditions. For instance, at the Dome Mine, Timmins, located close to the Porcupine Destor Fault, all of the vein quartz from five different mineralized domains has a

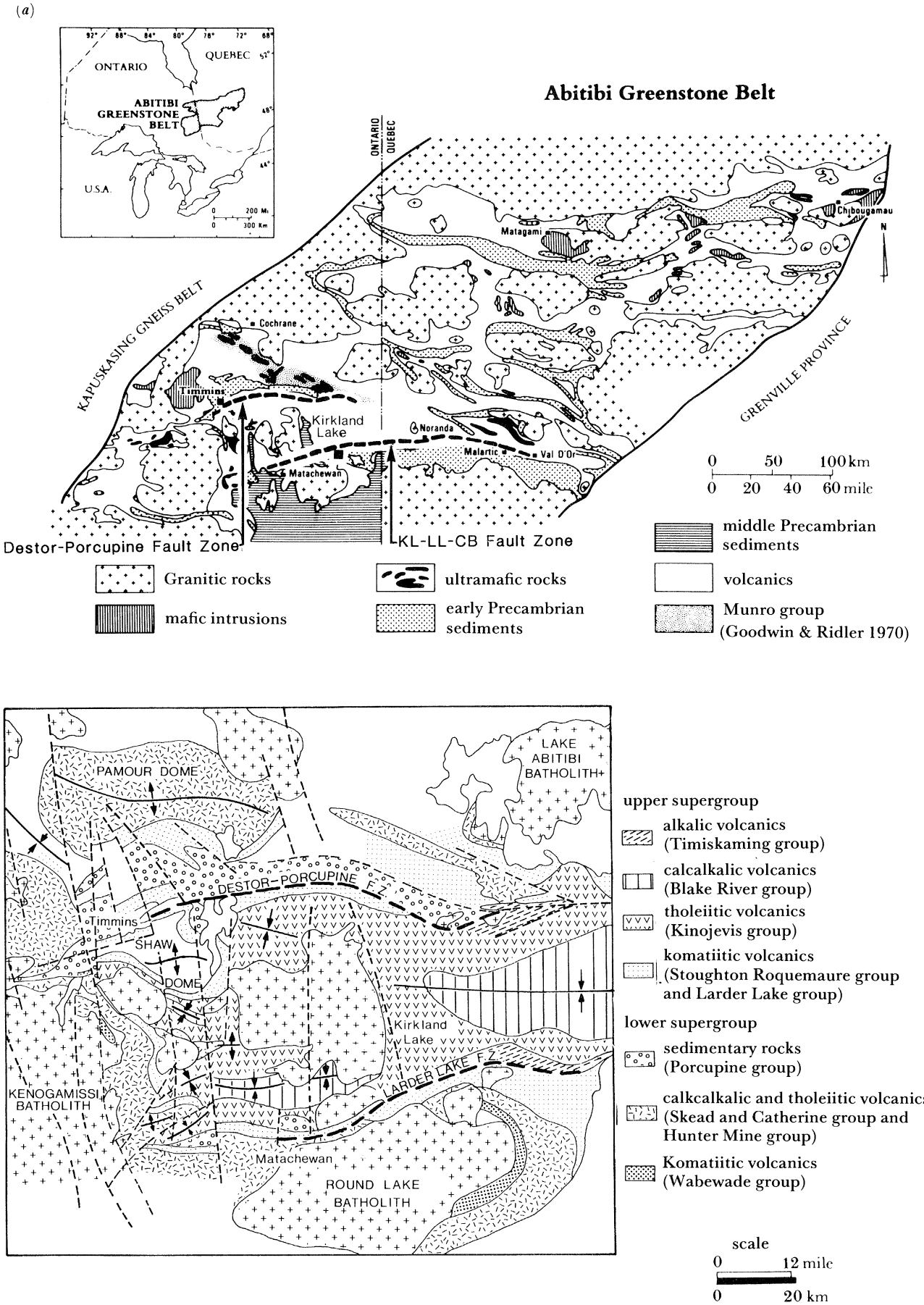

FIGURE 1. (*a*) Schematic geology of the Abitibi Belt (modified after Goodwin & Ridler 1970) KL–LL–CB is the Kirkland Lake–Larder Lake–Cadillac Fault Zone. (*b*) Geology of the Kirkland Lake area (after Jensen 1981).

restricted range of $\delta^{18}O$ values at 14–15.2: Δ(quartz–muscovite) and Δ(quartz–chlorite) are relatively constant at 3.5–4.0‰ and 5.5–6.1‰ respectively, corresponding to calculated isotopic temperatures at 270–450 °C, and a fluid isotopic composition of 7 ± 1‰.

Considering the data for fourteen mines collectively distributed over distances of several hundred kilometres along the two main fault systems, the overall estimated range of ambient fluid temperatures is 270–450 °C, with a fluid isotopic composition given by $\delta^{18}O = 6 \pm 2$ and $\delta D = -50 \pm 20$ (figure 2*a*). The fluid compositions are consistent with the range of most fluids implicated in metamorphism, and overlap the magmatic field, but are isotopically distinct from evolved marine or meteoric fluids (figure 2*a*; cf. Taylor 1974). The inferred metamorphic fluids, with a possible magmatic component, are considered to be generated during progressive accumulation and burial of the volcanic–sedimentary sequences, and hence were broadly contemporaneous with volcanic–plutonic activity.

The observed narrow interval of $\delta^{18}O$ (vein quartz) at 11–15 is independent of wall-rock lithology. Quartz in wall rocks is shifted from initial values towards that of vein quartz in proximity to zones of intense metasomatism. These relations signify fluid-dominated conditions along fault structures. A corollary of the above results is that lateral diffusion of chemical components such as CO_2, K, Au, etc., from wall rocks into fault zones (cf. Boyle 1961, 1979) is incommensurate with the isotopic data.

The ubiquitous presence of hydrothermal carbonates, along with quartz, in mineralized fault zones, provides evidence that the fluid reservoir carried significant CO_2, raising the question of the source of carbon. The oxygen and carbon isotope compositions of hydrothermal carbonates, principally from fault-hosted lode gold deposits, are summarized in figure 2*b–e*. For most data, carbonates occupy a restricted field, where $\delta^{18}O$ values span 10 to 17, and $\delta^{13}C$ spans -8 to -0.5.

In general, quartz–carbonate pairs are out of oxygen isotope equilibrium, probably because of the susceptibility of carbonates to retrograde oxygen exchange. The carbon isotope compositions define a narrow field compared with most hydrothermal systems. According to Ohmoto & Rye (1979), variations in the $\delta^{13}C$ values of hydrothermal carbonates may arise from temperature fluctuations, decreasing CO_2/CH_4 ratios of the fluids, and increasing contributions of CO_2 from other sources. If the redox state during carbonate precipitation in the fault zones was close to the Q.F.M. buffer, then $\delta^{13}C$ ($CaCO_3$) $\approx \delta^{13}C$ (fluid) (Ohmoto & Rye 1979).

Carbon with $\delta^{13}C$ of -8 to -0.5‰ could be derived from a number of different carbon reservoirs, given that the average $\delta^{13}C$ value of igneous, sedimentary and metamorphic rocks is *ca.* -5, and of juvenile carbon is -5 ± 2 (Ohmoto & Rye 1979). Kerrich (1983) and Golding & Wilson (1983) have argued on the basis of carbon isotope data and geological considerations that the hydrothermal CO_2 is derived from a mixture of juvenile carbon and marine carbonate. Fyon *et al.* (1984) propose a mantle origin for the CO_2. A contribution of carbon from oxidation or hydrolysis of low-^{13}C hydrocarbons in interflow sediments at source is also possible, to account for the most depleted values (figure 2*b–e*; Fyon *et al.* 1982, 1984; Kishida & Kerrich 1985). A key feature is the provinciality of $\delta^{13}C$ carbonate values (figure 2*b–d*). Redox-dependent fractionations accompanying the precipitation of carbonates account for at most a shift of -2‰, and some of the most depleted regions are in rocks essentially devoid of carbonaceous material. The observed provinciality is interpreted in terms of lateral

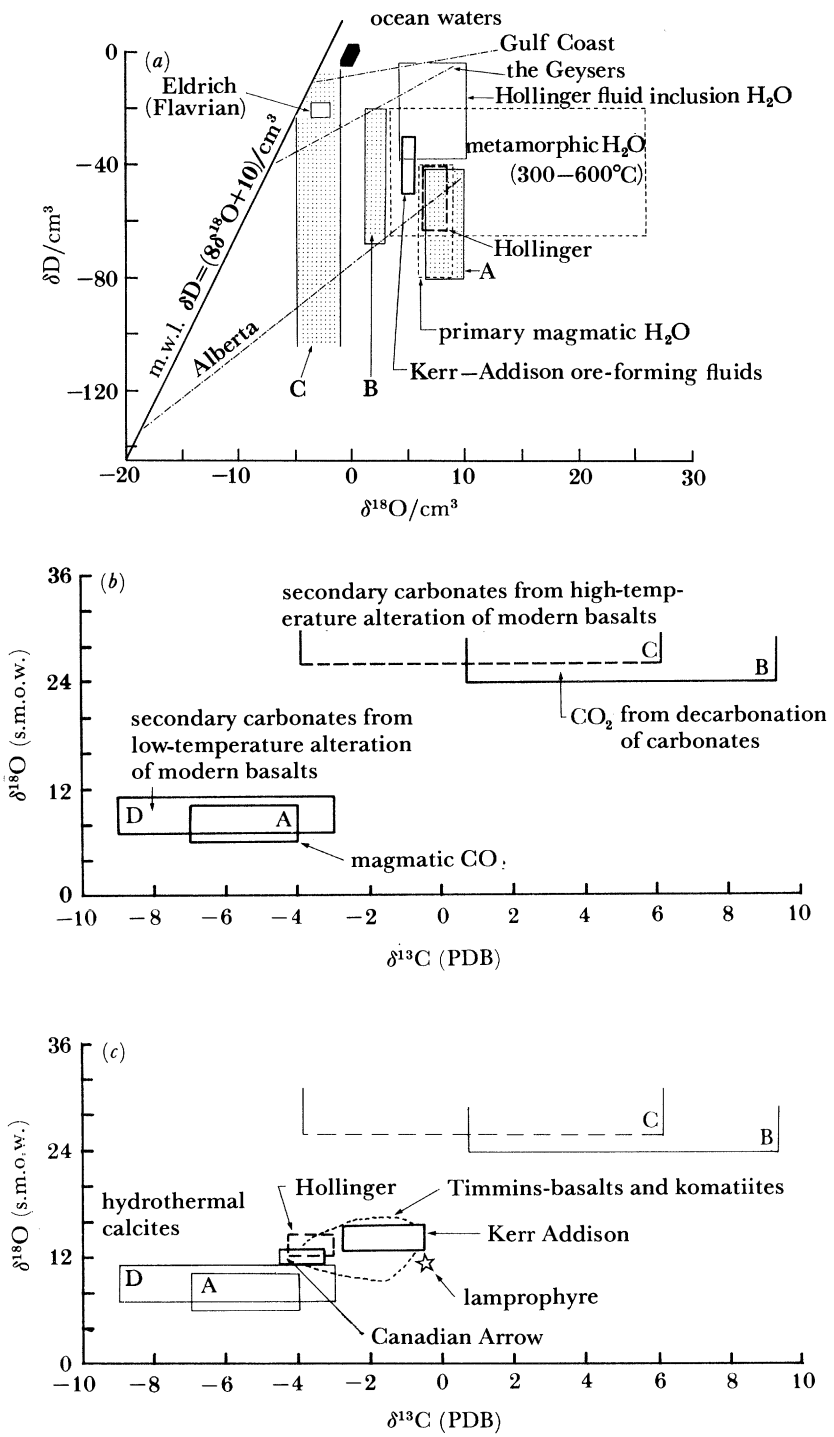

FIGURE 2 (*a–c*). For description see opposite.

heterogeneities in the lower crust supplying CO_2 to structures, represented by variations in the relative proportions of oxidized to reduced carbon.

Hydrogen sulphide is a minor volatile component of fault-related hydrothermal fluids, reflected in the presence of sporadic concentrations of pyrite ± arsenopyrite. The sulphur isotope

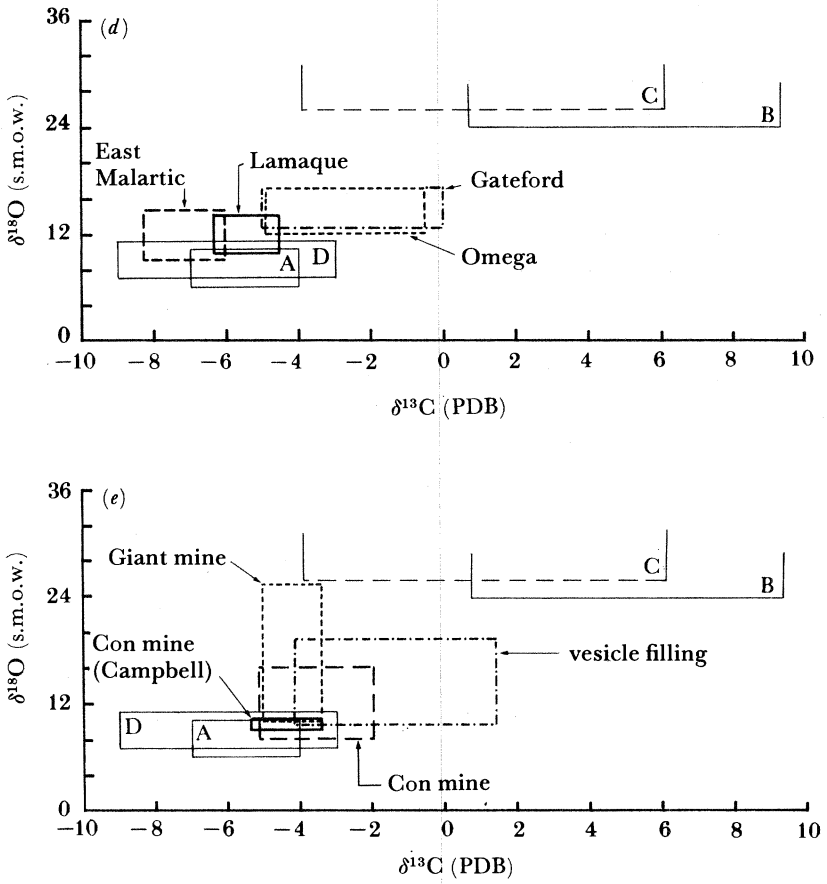

FIGURE 2. (*a*) Isotopic composition of natural terrestrial fluid reservoirs in δD, δ^{18}O coordinate space, modified after Taylor (1974). M.w.l. is the meteoric water line. Calculated fields for three vein stages at Macassa are superimposed: A, ore solutions; B, fluids associated with selenite deposition in faults; C, late-stage quartz–magnetite stringers (after Kerrich & Watson 1984); Hollinger (this paper); Kerr Addison (Kishida & Kerrich 1985); and Eldrich (Kennedy 1985). Data for H_2O deprepitated from quartz veins of the Hollinger Mine is from Fyon *et al.* (1983). (*b*) Fields of different carbonates, and CO_2 derived from specified sources, plotted in δ^{13}C versus δ^{18}O coordinate space (modified from Foy 1985; Fyon *et al.* 1983). (*c*) Isotopic composition of hydrothermal carbonates associated with gold deposits, from the Timmins area (after Fyon *et al.* 1983); Hollinger Mine (data this paper), Matachewan (Canadian Arrow) and Larder Lake (Kerr Addison) areas. Abitibi Greenstone Belt (see figure 1*a*, *b*). (*d*) Isotopic composition of hydrothermal carbonates associated with gold deposits from the Larder Lake (Gateford and Omega properties, Foy 1985), Malartic and Val d'Or areas (Lamaque Mine). Note the provinciality of δ^{13}C, probably signifying variation in proportions of various carbon donors in the source region. (*e*) Isotopic composition of hydrothermal carbonates associated with gold mineralization from the Con and Giant Mines, Yellowknife. Also illustrated is the field for early vesicle filling carbonates, probably associated with spilitization of the volcanics.

composition of pyrite from gold deposits of the Timmins camp occupies a restricted field given by $\delta^{34}S = 2.7 \pm 1.9$, signifying a well mixed reservoir and uniform redox conditions at precipitation. Such values may reflect sulphur derived from a magmatic sulphur reservoir, or leaching of sulphides generated by the redistribution of magmatic sulphur accompanying early marine-water alterations of igneous rocks. A redox-dependent fractionation exists for the isotopic composition of hydrothermal pyrites (Ohmoto & Rye 1979). At the Canadian Arrow deposit, located on a splay of the Porcupine Destor Fault, pyrite is depleted in ^{34}S ($x = -11.2 \pm 1.0$‰ 1σ, $n = 18$) relative to examples at Timmins. Schwarcz & Rees (1984)

suggest a well mixed sulphur reservoir to account for the uniformity of sulphur isotope compositions, coupled with relatively oxidizing conditions to yield the isotopically light values.

Evidence from fluid inclusions on the properties of hydrothermal solutions involved in the fault-zone mineralization is sparse, because of pervasive transgranular fracturing and intracrystalline deformation of vein minerals. Some of the fluid inclusion data is compiled in Kerrich (1983) and Colvine *et al.* (1984). Such fluids were of low salinity (less than 3% by mass of NaCl equivalent), contained minor quantities of reduced gas species such as CH_4, CO and COS, minor N_2, possessed relatively high K/Na ratios (*ca.* 0.10), and are characterized by variable CO_2 contents, probably signifying transient effervescence of CO_2 during decompression.

In the Timmins, Matheson, Kirkland Lake and Val d'Or regions of the fault systems, sulphates occur close to or within the structures. The sulphates, typically anhydrite or selenite, coexist with albite, magnesium chlorite, calcite and haematite. On the basis of stable isotope data and mineralogical considerations these domains have been interpreted as sites for incursion of Archaean marine water into submarine volcanic rocks (Kerrich & Hodder 1982; Kerrich & Fyfe 1983): ambient temperatures were 150–200 °C, and $\delta^{18}O$ (fluid) $= 0 \pm 1.5‰$ (figure 2*a*).

A third fluid régime is evident from stable-isotope data in plutonic rocks of the Kirkland Lake and Noranda districts. In these districts quartz–magnetite and quartz–chlorite veins were precipitated at temperatures of 120–250 °C from low-^{18}O meteoric water (figure 2*a*).

Thus cooling of the volcanic–plutonic complexes was initially dominated by ocean water in the submarine environment, with a transition to meteoric-water cooling as the Archaean volcanic terrain emerged above sea level. This scheme is corroborated by the presence of late fluviatile clastic sediments.

(*c*) *Age relations*

A tightly constrained chronological framework exists for volcanic–plutonic activity in the Timmins and Kirkland Lake areas of the Abitibi Greenstone Belt, based on the classic U/Pb isotopic model age determinations conducted by Krogh *et al.* (1982). However, the timing of fluid transport through the major structures and the source of solute components have remained controversial issues. Attempts have been made to place limits on the age of fluid discharge, by using incremental $^{40}Ar/^{39}Ar$ and Rb/Sr isochrons on some of the prominent mineralized fault domains.

In the Kirkland Lake area, the Hunter Mine group, located near the top of the lower supergroup, or first volcanic cycle, has been dated at 2710 ± 2 Ma. The Blake River group, near the top of the upper supergroup, or second volcanic cycle, has an age of 2703 ± 2 Ma (Nunes & Jensen 1980). These ages are from the upper concordia intercept applied to zircons, which probably represent minima given the absence of xenocrystic zircons. Collectively these data, which span the cumulative stratigraphy of volcanic cycles with an apparent thickness of *ca.* 35 km, signify a time interval of 7 ± 3 Ma for accumulation of much of the Kirkland Lake section of the Abitibi Greenstone Belt (table 1). In the Timmins district, volcanic activity spanned *ca.* 22 Ma, from 2725 to 2703 Ma (table 1).

Granitic batholiths are thought to be broadly contemporaneous with volcanic activity. Krogh *et al.* (1982) report that most batholiths have ages in the narrow interval 2675–2685 Ma (U/Pb isotopic ages on zircons). A lower age constraint on Abitibi belt igneous activity is provided by a Rb/Sr whole-rock isochron age of 2690 ± 93 Ma on the Matachewan diabase dyke swarm

PHILOSOPHICAL TRANSACTIONS OF THE ROYAL SOCIETY A MATHEMATICAL, PHYSICAL & ENGINEERING SCIENCES

Table 1. Age constraints, Abitibi belt

	age/Ma	source
Timmins		(Nunes & Pyke 1981)
lower supergroup (top)	2725±2	
upper supergroup (top)	2703±2	
Kidd Creek felsic host	2717±4	
Kirkland Lake		(Nunes & Jensen 1980)
Hunter Mine group	2710±2	
Blake River group	2703±2	
Timiskaming	—	
Noranda		—
Lake Dufault granodiorite	2701	
Abitibi batholiths	2675–2685	(Krogh *et al.* 1982)
Matachewan dykes	2690±93 ($^{87}Sr/^{86}Sr = 0.700 \pm 0.001$)	(Gates & Hurley 1973)

(Gates & Hurley 1973) which transects all rock types, batholiths and some of the structurally hosted mineralization in the Timmins–Kirkland Lake area.

Existing age determinations on gold mineralization in structural lineaments such as the Kirkland Lake–Larder Lake Fault Zone are principally Stacey–Kramers model Pb isotopic ages on galenas and leached co-existing pyrite, which define ages of 2656–2700 Ma (Franklin *et al.* 1983). Rb/Sr isochron data and incremental $^{40}Ar/^{39}Ar$ spectra yield closure times of 2550–2700 Ma (table 1; figure 3; Kerrich *et al.* 1984). The least disturbed isotopic systems are in good agreement with model Pb ages, whereas the younger ones reflect resetting during continued displacement along the major structures into the Proterozoic. For instance, the Kirkland Lake Fault Zone locally displaces Proterozoic Cobalt group sediments, which are in the order of 2250 Ma.

The hydrothermal muscovite from Kerr Addison, on the Kirkland Lake Fault Zone, is characterized by a clear diffusion loss configuration, which can be modelled by assuming that there have been two separate events affecting the structure since formation of the muscovite (figure 3*a*). The best fit age of growth is 2750±50 Ma: in this model 57% of the ^{40}Ar was lost at 2030 Ma, with a further 3% loss at 1280±240 Ma. The former event may reflect the last significant displacement increment on the fault zone, whereas the 1280 Ma plateau may correlate with Grenvillian activity. Complications involved in the interpretation of $^{40}Ar/^{39}Ar$ age spectra have been emphasized by Harrison (1983).

By using the above results in conjunction with field relations, dominant hydrothermal activity in Abitibi belt structural lineaments is interpreted to have occurred during an episode of major fracturing and ductile deformation which accompanied emplacement of granitic batholiths into the supracrustal sequences: hydrothermal mineralization was thus an integral part of the thermal and mechanical energy of the greenstone belt.

(*d*) *Source of the hydrothermal solutes*

The origin of fluid reservoirs which infiltrated structural lineaments has been considered above on the basis of light stable-isotope evidence. However, the source-rock reservoir for hydrothermally transported solutes, such as Si, CO_2, K, Rb, Li, Cs, Sr and rare metals including Au, Ag, As, Sb, B, Se, Te, Pb, Bi, W, etc., is a more subtle problem. Here, the question is explored by means of radioisotope tracers, namely $^{87}Sr/^{86}Sr$ and $^{207}Pb/^{204}Pb$, $^{206}Pb/^{204}Pb$, which may be diagnostic of the specific rock reservoir from which the solutes were derived.

PHILOSOPHICAL TRANSACTIONS OF THE ROYAL SOCIETY A MATHEMATICAL, PHYSICAL & ENGINEERING SCIENCES

Initial $^{87}Sr/^{86}Sr$ ratios of mineralized domains in major structures may be estimated by using Rb/Sr isochrons, and from analyses of Sr-rich, Rb-poor minerals that have plausibly acted as closed isotopic systems. Whole-rock Rb/Sr isotopic systems have been disturbed since the time of mineralization, probably because of continued displacement on major structures into the Proterozoic. However, the Rb/Sr isotopic data may be extrapolated backwards to estimate the $^{87}Sr/^{86}Sr$ ratio at the time of fluid transport, by rotating isochrons about the mean $^{87}Rb/^{86}Sr$ of mineralized rocks to the correct age, as independently determined by model Pb ages and lower age limits imposed by U/Pb dating on zircons (see above). For instance, by using a value of 0.70249 ± 0.0009 for $^{87}Sr/^{86}Sr$ at the time of closure (namely 2510 Ma), and an estimated age of 2690 for mineralization, the $^{87}Sr/^{86}Sr$ of fluids discharging through the fault would have been 0.7010 ($^{87}Rb/^{86}Sr = 0.038$) to 0.7015 ($^{87}Rb/^{86}Sr = 0.025$) (table 1).

Contemporaneous $^{87}Sr/^{86}Sr$ ratios of the hydrothermal mineralization have been independently estimated from analyses of tourmaline, scheelite and piemontite, all of which possess $^{87}Rb/^{86}Sr \leqslant 0.004$, and therefore have negligibly small radiogenic strontium evolution over the elapsed time since formation. Moreover, these minerals, unlike ferrodolomites present in the fault zones, appear to have behaved as isotopically closed systems. Strontium isotope data for mineralized fault zones are compiled in table 2. Initial strontium isotope ratios for the fault mineralization are probably those of the hydrothermal fluids which donated Sr, and this may also reflect the $^{87}Sr/^{86}Sr$ of the rock reservoir with which the fluids equilibrated.

TABLE 2. Rb/Sr ISOCHRON AND $^{40}Ar/^{39}Ar$ CLOSURE AGES FOR MINERALIZED FAULTS, AND AGE-CORRECTED MINERAL $^{87}Sr/^{86}Sr$ RATIOS

district mine	age/Ma	method	$^{87}Sr/^{86}Sr$ (initial)	$^{87}Sr/^{86}Sr$ (age-corrected)	$^{87}Sr/^{86}Sr$ (mineral) (age-corrected)
Timmins					
Hollinger	2440 ± 26	Rb/Sr	0.70262 ± 0.0014	0.7015	—
	2570 ± 30	$^{40}Ar/^{39}Ar$ (muscovite)	—	—	—
Parnour	—	—	—	—	0.7010 t
Paymaster	—	—	—	—	0.7012 to 0.7015 t
Aunor	—	—	—	—	0.7014 to 0.7020 t
Dome	—	—	—	—	0.7015 t, s
Kirkland Lake					
Macassa	2575 ± 50	$^{40}Ar/^{39}Ar$ (actinolite)	—	—	0.7012 to 0.7011 a, s
Kerr Addison	2510 ± 50	Rb/Sr	0.70249 ± 0.0009	0.7010	—
	2550 ± 40	$^{40}Ar/^{39}Ar$ (muscovite)	—	—	—
Bousquet					
Dumagami	2420 ± 19	Rb/Sr	0.70406 ± 0.0001	0.7020	—
	2550 ± 30	$^{40}Ar/^{39}Ar$ (muscovite)	—	—	—
Bousquet	—	—	—	—	0.7017 to 0.7019 t
Val d'Or					
Lamaque	—	—	—	—	0.7031 to 0.7041 t
Pascales	—	—	—	—	0.7007 to 0.7014 t
Bras d'Or	—	—	—	—	0.7010 to 0.7022 t

t, tourmaline; s, scheelite; a, actinolite.

If the estimated ratio range of 0.7011–0.7040 for the source-rock reservoir of hydrothermal solutes has validity, then this reservoir was more radiogenic than the upper mantle at 2690 Ma (0.700 ± 0.001), the Matachewan diabase dyke swarm (0.701 ± 0.001), or contemporaneous Abitibi belt volcanics of mafic to ultramafic composition (0.7000 to 0.7012; see tables 1, 2; figure 4; Faure 1977; Gates & Hurley 1973; Hart & Brooks 1974; figure 3*a*). An inferred radiogenic

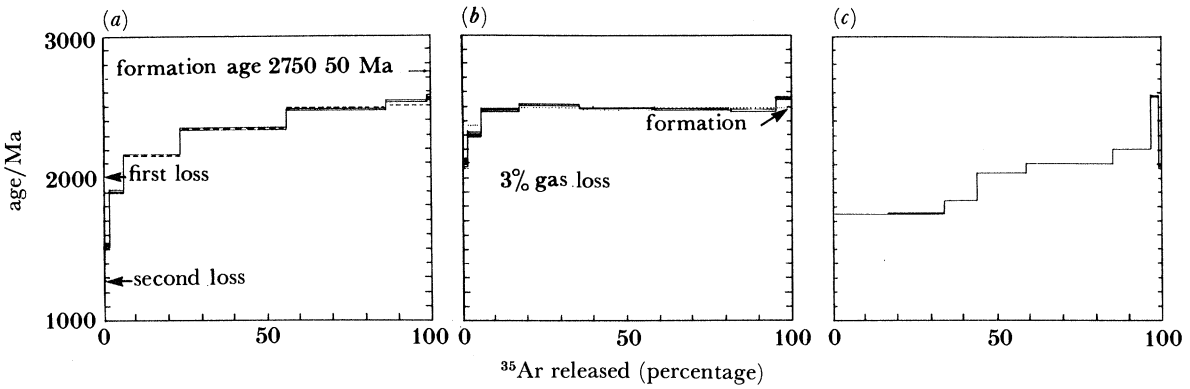

FIGURE 3. Incremental $^{40}Ar/^{39}Ar$ spectra from fault-related hydrothermal minerals. (*a*) Kerr Addison muscovite (AK 44 sericite); (*b*) Dumagami muscovite (D 48 muscovite); dotted line shows single-loss model; (*c*) Macassa actinolite (G 80–88 actinolite).

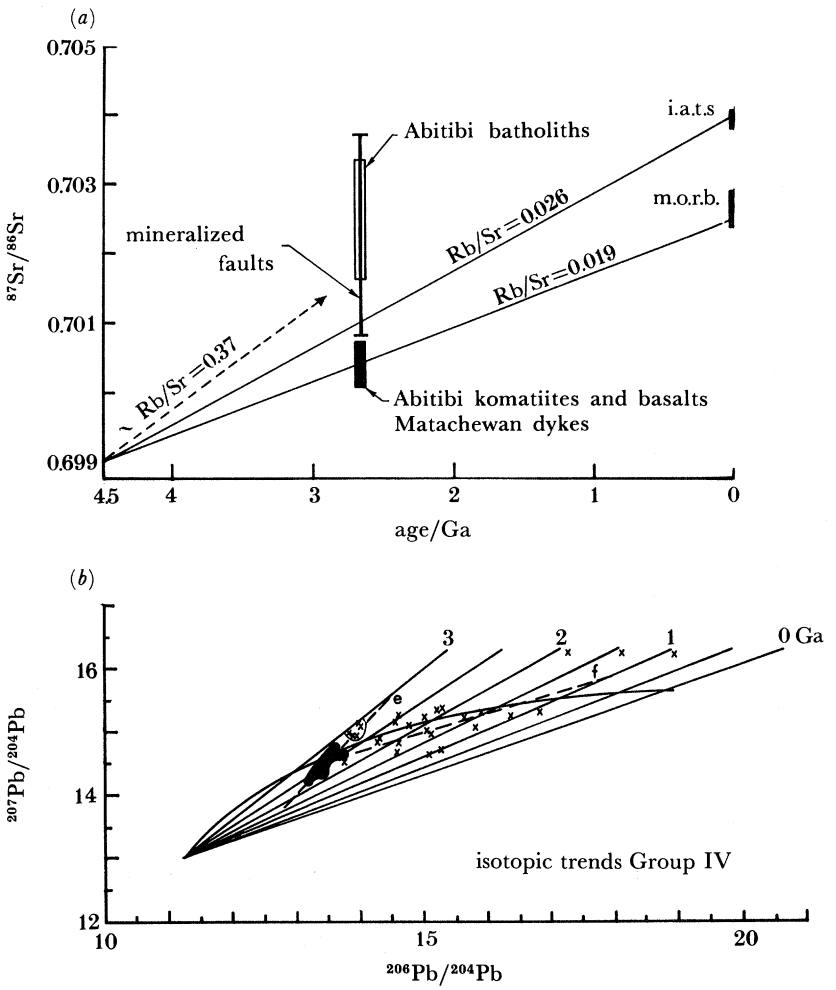

FIGURE 4. (*a*) Contemporaneous $^{87}Sr/^{86}Sr$ of mineralized linear structures, compared with mantle, komatiites, and grandodiorite batholiths, for the Abitibi Greenstone Belt at 2.7 Ga. (*b*) Lead isotopic composition of massive sulphides (solid) and mineralized structures (crosses), after Franklin *et al.* (1983).

character for the source may implicate contributions from sialic basement to the greenstone belt, or felsic volcanic rocks of the Lower Supergroup, as well as volatiles released from the mafic to ultramafic volcanic sequence. Franklin *et al.* (1983) have shown on the basis of lead isotopic work that, in general, fault-hosted gold mineralization in the Abitibi Greenstone Belt possesses a characteristically more radiogenic signature and higher μ than contemporaneous mafic volcanic rocks.

Thus the deduced Sr and measured Pb isotopic character of the fault mineralization are more evolved than their contiguous mafic volcanic-bounding media, collectively implicating a deeper-level, more radiogenic source for these components. This source is probably the same as that donating Si, CO_2, K, Rb, Li, Cs, Au, Ag, As, Sb, B, etc. Long-range communication to a deep crustal source is corroborated by the presence of the major structures themselves, as well as independent estimates of transport distances based on enrichments of rare elements in the structures (Kerrich & Fryer 1979; Kerrich 1983). A distinct provinciality of $^{87}Sr/^{86}Sr$ initial ratios exists (table 1), and as for $\delta^{13}C$, this is interpreted in terms of lateral heterogeneity of the lower crust supplying volatiles and solutes to the structures.

(*e*) *Mineralogical constraints on fluid chemistry*

Mineral assemblages of metasomatized fault zones vary considerably, but in general the characteristic species are quartz plus carbonate, along with subordinate muscovite, albite, chlorite, talc, tourmaline, scheelite and sulphides or arsenides. The relative proportions of minerals and their composition depend critically on the lithology which faults intersect. For instance, where structures traverse granitic rocks the dominant carbonate is calcite, whereas in tholeiitic basalts and ultramafic rocks, ferroan dolomite and magnesite predominate respectively. Similarly, hydrothermal chlorite and muscovite may contain a small percentage of Cr in faults hosted by ultramafic flows, whereas their counterparts in structures propagating through felsic rocks possess low Cr abundances.

In general, hydrothermal fluids venting through fault zones donated volatiles and potassium, with wall rocks contributing bivalent metal cations. Thus hydrothermal carbonates reflect the carbonation of Fe, Mg and Ca silicate precursors such as chlorite and epidote to Fe, Mg and Ca carbonates; hydrothermal muscovite or potassium feldspar represent the hydrolysis of chlorite with addition of aqueous potassium; and pyrite represents the transfer of Fe from a silicate or oxide reservoir to sulphide minerals accompanying the consumption of H_2S.

Progressive mineralogical reactions of these types, involved in hydrothermal alteration of Fe tholeiites and ultramafic rocks along the Kirkland Lake Fault Zone, have been studied in detail by Kishida (1984). Such reactions can be evaluated in terms of T, X_{CO_2}, $a(K^+/H^+)$ and $a(Na^+/H^+)$, according to equilibria given by Montoya & Hemley (1975). Two reactions are considered here, namely

$$\text{chlorite} + \text{calcite} + CO_2 \rightarrow \text{ankerite} + \text{muscovite} + \text{quartz} \qquad (1)$$

and

$$\text{chlorite} \rightarrow \text{muscovite} + \text{albite} \qquad (2)$$

(see figures 5*a*, *b*). Reaction (1) depends on small changes of X_{CO_2} and $a(K^+/H^+)$, whereas reaction (2) is mediated by $a(K^+/H^+)$ but is independent of X_{CO_2}. Assuming a temperature of 300 °C coupled with isothermal conditions, a value of $a(Na^+/K^+) \geqslant 10{:}1$ can be deduced for (carbonate + albite + muscovite) alteration (cf. Montoya & Hemley 1975).

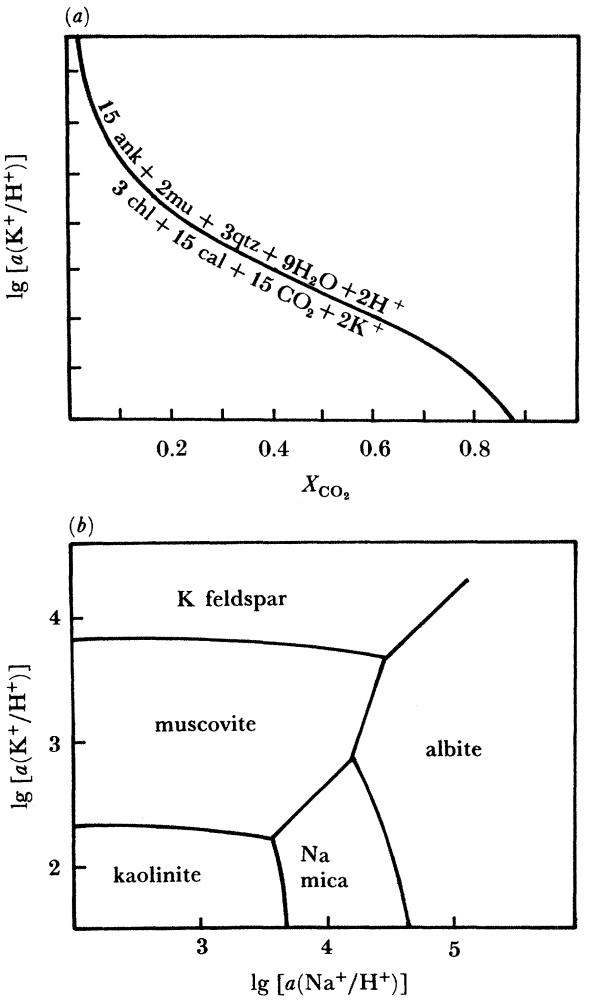

FIGURE 5. (*a*, *b*) Equilibria relations for specified reactions (after Montoya & Hemley 1979), as applied to mineralized fault zones of the Abitibi Belt (cf. Kishida 1984); ank, ankerite; mu, muscovite; qtz, quartz; chl, chlorite; cal, calcite.

From these considerations it can be deduced that the fluids responsible for the specified hydrothermal mineral assemblages along the Kirkland Lake Fault were characterized by $X_{CO_2} = 0.1$, a neutral to slightly acidic pH, and aqueous $Na^+/K^+ = 10:1$.

(*f*) *Fluid volumes–solute concentrations*

The total production of gold from the Porcupine district up to 1976 was 1.7×10^9 g (Pyke 1976). It is assumed that this mass of gold was derived by 50% efficient leaching of metabasalts with an average Au abundance of $2/10^9$ (by mass) (Tilling *et al.* 1973; Kwong & Crocket 1978), then the source volume would be of the order of 600 km^3 (1 km^3 of rock contains 5.6×10^6 g Au at $2/10^9$). Based on the premise that Si, Au, Aq, Pd, W, Ni and Cr, together with other elements present in veins, were leached and transported during metamorphic outgassing within the greenschist facies or at the greenschist–amphibolite transition, when approximately 5% (by mass) structural water is released from a hydrated rock of basaltic composition, then the solvent volume would be of the order of 90 km^3.

An independent estimate of the hydrothermal fluid volume may be derived as follows, with the use of gold-bearing quartz veins (which are essentially pure quartz) as examples. In cooling from 550 to 300 °C, 1 kg of quartz-saturated water will precipitate 2.6 g of quartz, assuming a thermal gradient of 100 °C km^{-1} and a hydraulic gradient equal to the lithostatic gradient (Holland & Malinin 1979). Gold is present in the veins at an average level of $10/10^6$ (by mass), and therefore if gold and quartz were coprecipitated from a solution cooling along a geothermobar, then 1 kg of solvent would precipitate 2.6×10^{-5} g Au, and the average decrease in concentration of gold in the hydrothermal solution would be 25 ng ml^{-1}. The total carrier fluid volume for 1.7×10^9 g Au is then 65×10^{12} kg (65 km^3), based on the generalized assumption that gold is dominantly precipitated over the stated temperature interval. Estimates of fluid volume are slightly increased if a lower thermal gradient is assumed or if CO_2 consumption from the hydrothermal fluid acts to decrease the rate of change of silica solubility during cooling. Furthermore, consider 100 g of metabasalt containing Au at $2/10^9$. If 50% of the gold is taken into solution as the metabasalt evolves 5% (by mass) water at the greenschist–amphibolite transition, then the solute concentration will be 20 ng ml^{-1} Au ($20/10^9$), which is comparable to the figure estimated above and the value of 50 ng ml^{-1} reported by Tilling *et al.* (1973) for gold in natural thermal waters. These calculations are intended to demonstrate the magnitude of source and fluid volumes, and provide estimates of Au concentrations. Similar calculations on gold transport are given by Helgeson & Garrels (1968) and Fyfe & Henley (1973).

Seward (1979) reports deposition of ore-grade gold material, along with Ag, Sb, Hg and Il, from dilute fluids with $1000/10^6$ (by mass) chloride, $0.04/10^9$ Au and $0.7/10^9$ Au in the Wairiki geothermal system, New Zealand. For fluids carrying $0.04/10^9$ Au, 800 km^3 of hydrothermal solution would contain 28000 kg gold. Although these solute concentrations for gold in a modern system are about one hundred times lower than the maximum values calculated above for the higher temperature Archaean vein deposits, and the values determined by Tilling *et al.* (1973), they serve to illustrate that high metal concentrations in hydrothermal fluids are not necessary to form ore-grade deposits.

(*g*) *Sodic and alkaline igneous rocks*

A characteristic feature of the major fault zones are sporadically distributed collinear arrays of subvolcanic stocks along with their extrusive equivalents of highly sodic or alkaline composition. Prominent examples include trondhjemites of the Malartic, Matachewan and Timmins areas, and alkaline rocks at Kirkland Lake (figure 1*a*, *b*).

The sodic rocks conform in most respects to the definition of a trondhjemite based on major element oxides, according to Barker (1979): namely SiO_2 exceeding 68%, but usually less than 75%, Al_2O_3 typically more than 15% at 70% SiO_2 and less than 14% at 75% SiO_2, and Na_2O at 4.0–5.5%. For instance, a population of six trondhjemites at Canadian Arrow possess $SiO_2 = 65.9 \pm 1.8\ 1\sigma$, $Al_2O_3 = 16.7 \pm 0.22$, and $Na_2O = 8.32 \pm 1.16$ (McNeil & Kerrich 1986). Most such trondhjemites have elevated primary Na_2O contents, but this is incremented during pervasive spilitic alteration in the presence of marine water, under conditions of low temperature, as shown by reversed quartz–feldspar fractionations $\delta^{18}O$ (quartz) = 9–11, $\delta^{18}O$ (albite) = 10–16, Fryer *et al.* 1979; Kerrich & Fryer 1979; Kerrich 1983). A general concensus exists that such magmas form by partial melting of mafic granulites at the base of the greenstone belt sequence (Collerson & Fryer 1978; Barker *et al.* 1979).

PHILOSOPHICAL TRANSACTIONS OF THE ROYAL SOCIETY A MATHEMATICAL, PHYSICAL & ENGINEERING SCIENCES

Groups of alkaline igneous intrusions and trachytic tuffs at Kirkland Lake are characterized by SiO_2 in the range 48–56 %, and K_2O in the range 5.5–9.8 %. Relatively abundant ilmenite, hornblende or augite is reflected in elevated TiO_2, Fe_2O_3, MnO, CaO and MgO contents, along with high concentrations of mafic-affiliated elements such as V, Cr, Co, Ni and Sc.

Formerly termed syenites, these rocks are in fact potassic basalts and intrusive equivalents. Specifically the low absolute Zr and Nb abundances result in high Ti/Zr ratios (13–35) for syenites, where Ti/Zr is typically about 7, and Nb/Y ratios of 0.2–0.5, which are smaller by a factor of 5–10 than is typical of syenitic rocks (Kerrich & Watson 1984). Moreover, the Ti/V, Zr/Y, K/Rb and Rb/Sr ratios are lower, and the Cr/Ni ratios higher, than for most rocks of syenitic composition. Rare earth element distributions for unaltered samples of the alkaline rocks are remarkably uniform (figure 6), defining a coherent array with chondrite-normalized

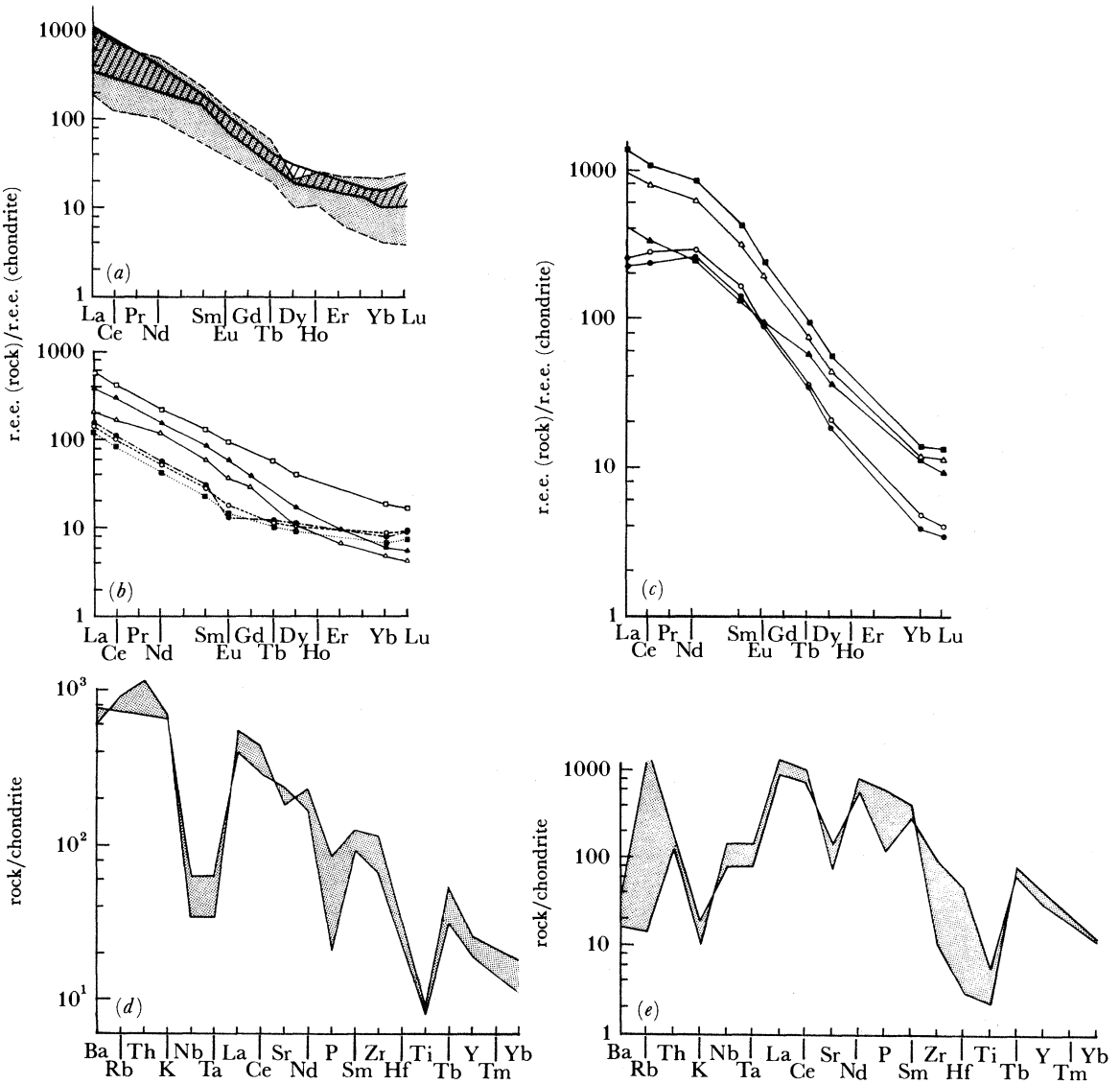

FIGURE 6. Chondrite-normalized element distributions for specified suites of alkaline magmas. (*a*) Lamprophyres (calc-alkaline lamprophyre envelope) (after McNeil & Kerrich 1985); (*b*) alkali-basalts (after Kerrich & Watson 1984); (*c*) fluorapatite-bearing fenitized trondhjemites (King & Kerrich 1986); (*d*) trachytes from Kirkland Lake; (*e*) fluorapatitive-rich fenites (King & Kerrich 1986).

La at 100–200, and the h.r.e.e. *ca.* 10 times the chondritic abundances. A characteristic feature of these rocks is the pronounced chondrite-normalized troughs at Ta/Nb, P and Ti (figure 6*c*).

There is a general concensus that alkaline mafic rocks are the products of low degrees of partial melting of asthenosphere, or 'enriched' asthenosphere, and such fusion products may have a preferred spatial association with linear fracture zones, such as rifts (cf. Fitton 1986, this symposium). Along with the alkaline magmas are lamprophyric dykes and domains of fenitization, highly enriched in large-ion lithophile elements. Representative chondrite-normalized diagrams are depicted in figure 6*a–e*.

The spatial association of trondhjemites and alkaline magmas with major linear structures is interpreted in terms of translithospheric fractures, which tap magmas of sodic composition generated at the base of the crust, and deep asthenospheric partial melts of alkaline composition. Such magnatic activity is broadly coeval with venting of hydrothermal fluids, probably from a crustal reservoir.

3. Fluid régimes in fault and shear zones, Yellowknife

(*a*) *Geological setting*

The Yellowknife Greenstone Belt, juxtaposed against the Western grandodiorite – an intrusion of batholithic proportions, is notable for a series of large-scale brittle–ductile shear zones locally containing gold lodes, displaced by a NNW-trending array of mineralized major faults (figure 7). This section addresses questions of fluid flow and chemical transport within these large-scale structures, which traverse both the mafic volcanic sequence and margins of the batholith.

The largest shear zones, the Con, Campbell and Giant, are exposed for distances up to 70 km, are 10–150 m wide, and extend to depths of more than 1–2 km (figure 7). These shear zones transect metabasic volcanic rocks and interflow metasediments at angles of 20–70° in the vertical plane. The geometrical relations of minor structures indicate that the shear zones conform to the simple shear model of Ramsay & Graham (1970). By using this model, and assuming an average width for the Campbell Zone of 80 m, the maximum computed displacement is about 300 m, west side up (cf. Kerrich & Allison 1978).

After initial development of the shear zones, these structures acted as permeable conduits for episodic discharge of hydrothermal fluids, which precipitated gold-bearing quartz–carbonate veins. The structures and ore bodies contained in them have been described by Boyle (1961), Henderson & Brown (1966), Breakey (1975) and Kerrich & Allison (1978). Shear zones in the granodiorite have a geometry and attitude that is essentially congruent with that of shear zones in the metabasalts and for which a similar sense of displacement and timing is indicated.

(*b*) *Unmineralized structures*

In traverses across unmineralized sections of the Campbell and Con Shear Zones, from isotropic epidote–amphibolite facies metabasalts through to deformed chlorite schists, the whole-rock $\delta^{18}O$ values remain approximately constant at 7–7.5‰, and $Fe^{2+}/\epsilon Fe$ is constant at *ca.* 0.7 V (figure 7*c*). These data are interpreted to indicate that deformation took place under conditions of low water/rock ratio (see also Kerrich & Fyfe 1981). The overall hydration accompanying initial development of shear zones is interpreted to result from volume dilation during an early phase of brittle fracture preceding development of a ductile fabric (cf. Kerrich

PHILOSOPHICAL TRANSACTIONS OF THE ROYAL SOCIETY A MATHEMATICAL, PHYSICAL & ENGINEERING SCIENCES

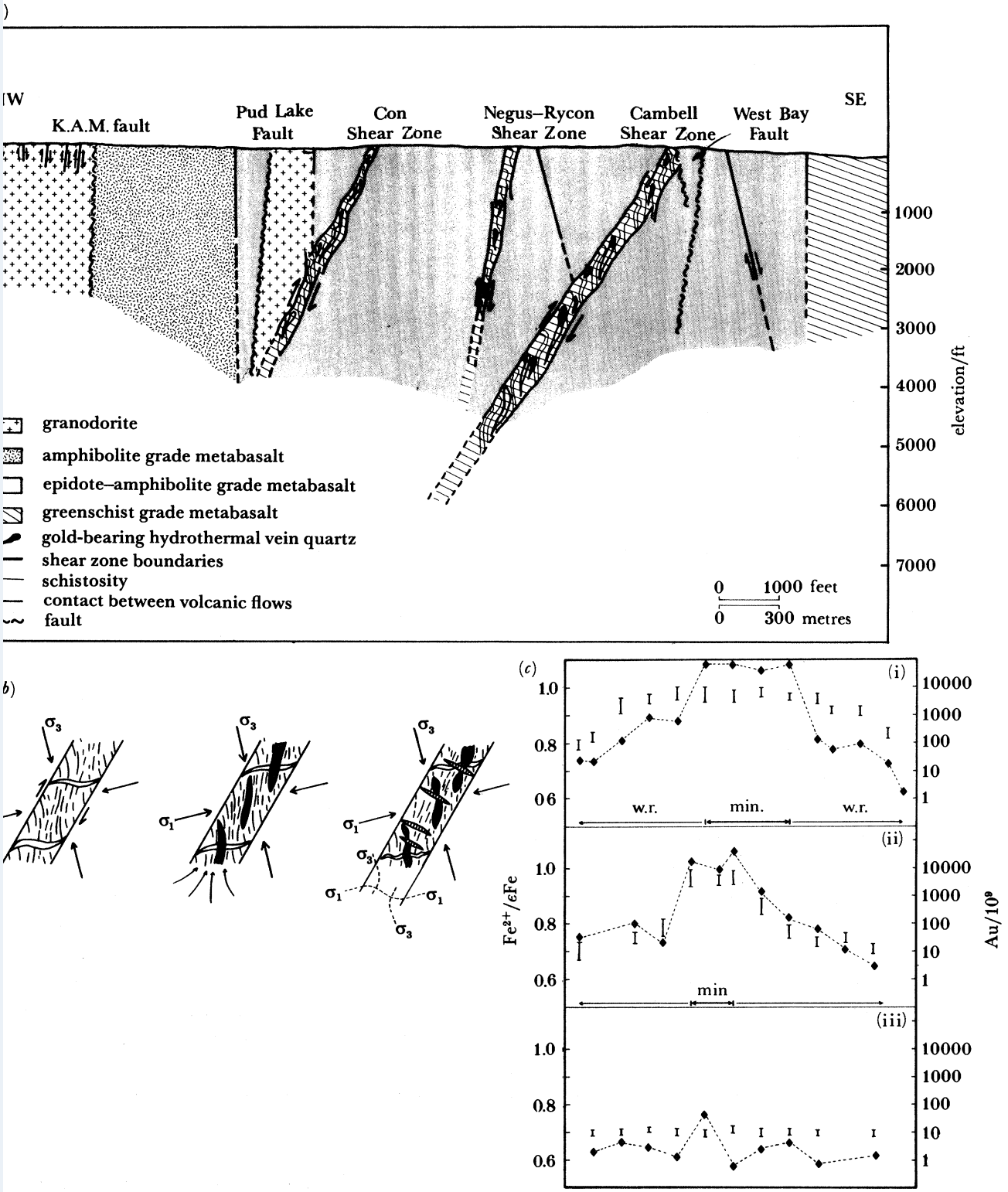

FIGURE 7. (*a*) Schematic geological cross section of the Yellowknife Greenstone Belt, illustrating the disposition of the principal rock types, and geometry of the brittle–ductile shear zones. (*b*) Possible switching of stress régimes accompanying hydraulic fracturing the generation of the three sets of vein arrays (after Kerrich & Allison 1978). (*c*) Variations in redox state and gold abundance across mineralized and barren shear zones; gold shown by bars, redox state by diamonds; (i) large-scale vein in shear zone; (ii) small-scale vein in shear zone; (iii) barren shear zone; w.r., wall rock; min, domain of high-grade mineralization.

& Allison 1978), with migration of pore fluids indigenous to the surrounding rocks into the structures.

Taylor (1968) has shown that fresh, unaltered submarine basalts have whole-rock $\delta^{18}O$ values of 5.7–0.3‰. The slight enrichment in ^{18}O recorded for these volcanic rocks relative to primary submarine basalts is attributed to oxygen isotope exchange with sea water at low temperatures, during thermally driven convective cooling of the ocean crust before development of the shear zones.

(*c*) *Mineralized shear zones*

Along discrete conduits within the shear zones, chlorite schists have transformed to chlorite–carbonate–muscovite–quartz–pyrite schists in envelopes around massive gold-bearing quartz veins. In close proximity to these veins, the whole-rock $\delta^{18}O$ values and $Fe^{2+}/\epsilon Fe$ exhibit a major perturbation from background values of 7‰ and 0.7, respectively (with Au less than $4/10^9$), to 9–10‰ and an average $Fe^{2+}/\epsilon Fe$ of 0.92 V in carbonate–sericite schists enveloping Au-bearing quartz veins (Au $1–40/10^6$) (figure 7*c*). The $\delta^{18}O$ of vein quartz is equal to that of quartz extracted from the carbonated mafic schists, implying oxygen isotope equilibrium between hydrothermal fluids and altered wall rocks under conditions of high water/rock ratios.

In general, studies of metamorphic processes indicate that ferrous/ferric ion ratios undergo little change during regional metamorphism, but this is not so for environments where high water/rock ratios were involved. Oxidation–reduction reactions under high-temperature metamorphic conditions occur mainly in response to the dissociation of water, according to the reaction $2H_2O \rightarrow 2H_2 + O_2$. Note that for an aqueous fluid at high temperatures, the equilibrium $P_{H_2} \gg 2P_{O_2}$ on account of reactions of the type (Fe^{2+} silicate) + $H_2O \rightarrow$ (Fe_3O_4 silicate) + H_2. The predominance of Fe^{2+} in mineralized wall rocks is thus believed to result from the reduction of Fe^{3+} in silicates and metal oxides by hydrogen during interaction with a large flux of H_2-bearing aqueous solutions ascending along a temperature–pressure gradient through conduits within the shear zones.

Minimum integrated water/rock ratios of more than 3:1 are indicated by the shift in redox state, and values in excess of 30:1 may be deduced from the abundance of quartz and quartz-solubility relations. Considerations of gold concentration from background into the veins reveals that a minimum of 9 km^3 of hydrothermal solutions discharged through the structures.

Ambient thermal conditions during fluid transport and mineralization are estimated at 400 ± 30 °C based on mineralogical and oxygen isotope data. If the ambient mineralization temperatures of 370–430 °C derived above are broadly correct, then the calculated $\delta^{18}O$ values of fluids from which the veins were precipitated is 6–8‰. These values are consistent with the range in $\delta^{18}O$ of fluids implicated in metamorphism, and overlap the primary magmatic range (Taylor 1974). Quartz $\delta^{18}O$ values are in general 1.5‰ lighter and temperatures *ca.* 100 °C hotter in the high water/rock ratio mineralized domains, compared with barren low water/rock ratio counterparts, commensurate with transport of high-temperature fluids from depth up the structures.

(*d*) *Western granodiorite*

In the internal regions of the Western granodiorite batholith, rocks are generally characterized by a primary igneous mineralogy. Whole-rock $\delta^{18}O$ values of 7.8–8.4‰, combined with quartz $\delta^{18}O$ values of 9.7–10.8‰ places these rocks within the class of isotopically 'normal' granitic rocks of Taylor (1978), defined as 6–10‰. Pegmatites within the batholith have quartz $\delta^{18}O$

values in compliance with that of quartz in the host rock, signifying common retention of a magmatic signature (Kerrich *et al.* 1984).

Traversing towards the batholith periphery, near the greenstone contact, the whole-rock and quartz $\delta^{18}O$ values progressively increase to 11 and 13.7‰ respectively. The enrichment in ^{18}O correlates with appearance of a retrograde greenschist facies mineralogy together with higher precious-metal contents (8–120/10^9 Au). Where shear zones formed in the interior regions of the batholith, no discernible shift in isotopic composition accompanying deformation was detected. However, towards the pluton boundary, undeformed granodiorite, its deformed product in shear zones, together with quartz veins emplaced in these structures, all record $\delta^{18}O$ (quartz) values of 12.1–13.7‰. These elevated values relative to the batholith interior, are close to that of second-generation vein quartz in shear zones transecting the neighbouring metabasalts. The results may be collectively interpreted in terms of a single fluid reservoir, with highly focused discharge through shear zone conduits within the metabasalts, but lower fluxes and less focused streaming through the adjacent batholith margin.

(*e*) *West Bay Fault*

The West Bay Fault is a major NNW-trending structure of unknown magnitude or direction of displacement (for a discussion see Boyle 1961). Locally the fault zone contains white massive quartz–haematite veins along with their brecciated products. Quartz $\delta^{18}O$ values of the veins ranges from 11.4–12.6‰. It is difficult to establish the temperature of quartz precipitation in the fault. From the quartz $\delta^{18}O$ values and temperature estimates of 240–320 °C, fluids streaming through the fault zone and precipitating quartz would have had an oxygen isotope composition of 2–6‰. The isotopic results are compatible with flow of several possible reservoirs, including formation brines, or mixtures of low-temperature metamorphic fluids, formation brines and surface waters. The presence of haematite signifies relatively high redox conditions, implying that a component of oxidizing surface waters was involved.

4. The Grenville Front

The Grenville Front, near Coniston, Ontario, is defined by the Grenville Front boundary fault and associated mylonite zones. These structures collectively form the demarcation between low-grade metasediments of the Southern Province and high-grade Grenville gneisses (La Tour 1981). Translation on the fault zone is thought to be of Grenville age (*ca.* 1 Ga), although the magnitude and direction of displacement are not precisely known. Bordering these structures immediately to the north is a major fault, the Wanapitae.

La Tour (1981) has distinguished two discrete and distinct mylonite zones at the Grenville Front, designated MZI and MZII. Metamorphic reactions associated with MZII are prograde in nature. On the basis of garnet–biotite geothermometry the ambient temperature of deformation is estimated at 600 °C, and oxygen isotope fractionations (Δ(quartz–muscovite) = 2.6–2.8/cm^3) yield temperatures of 580–640 °C, in close accord with the above (Kerrich *et al.* 1984). The $\delta^{18}O$ of quartz in mylonitic schists is uniform at 11.0–11.8; syntectonic quartz veins have $\delta^{18}O$ values within the same range as quartz in the host rock, signifying growth of veins in isotopic equilibrium with schists, and probably from the same fluid. Fluids present during syntectonic veining and deformation have calculated $\delta^{18}O$ values of 9.6 ± 0.2.

Metamorphic reactions in mylonite zone MZI are exclusively retrograde in nature, and

garnet amphibole thermometry indicates that deformation occurred at temperatures below 540 °C (La Tour 1981*a*). Oxygen isotope data for MZI yields temperature estimates of 420–490 °C, and fluid isotopic compositions of 7.0 ± 0.6‰. Fluids present during deformation along MZII and MZI were probably of metamorphic origin, indigenous to the immediate host rocks.

Rock units transected by the Wanapitae Fault have undergone extensive brittle fracturing, accompanied by local quartz–albite–carbonate veining. Oxygen isotope data on cataclastically deformed metadiabase yields temperature estimates of 280 ± 40 °C, and a fluid $\delta^{18}O$ value of 3.2. Fluid involvement in the Wanapitae Fault was at relatively low temperatures, possibly from a reservoir of formation brines (Kerrich *et al.* 1984).

An array of quartz–hematite veins ($\delta^{18}O$ (quartz) $= -0.8$ to -1.3) occupy fractured arrays superimposed on the mylonitic fabric of MZI. Quartz crystallized at temperatures of 200–350 °C in the presence of low-^{18}O fluids with an isotopic composition of -8‰ (350 °C) to -14‰ (200 °C). Continental meteoric water is the only terrestrial fluid reservoir with a negative $\delta^{18}O$ value. The fluid $\delta^{18}O$ values calculated above are commensurate with that of precipitation on high mountain ranges at medium to high latitudes, such as the Sierra Nevada, Rocky or Andean mountains (cf. Taylor 1974). This episode of fracturing is thought to have resulted from infiltration of low-^{18}O waters derived from precipitation on a high mountain range, down a brittle fault zone. The mountain range could have been induced by continental collision, with deformation accompanying crustal thickening accommodated at deep levels by translation on the high-temperature mylonite zone MZII, followed by isostatic rebound on the low-temperature zone MZI and the associated Grenville Front boundary fault (La Tour 1981*a*; Kerrich *et al.* 1984; figure 8). This scheme could account for the tectonic juxtaposition of high-grade gneisses deformed in a ductile mode in the presence of metamorphic fluids at elevated temperatures, with low-grade metasediments that had experienced brittle fracturing during the incursion of an ^{18}O-depleted surface reservoir.

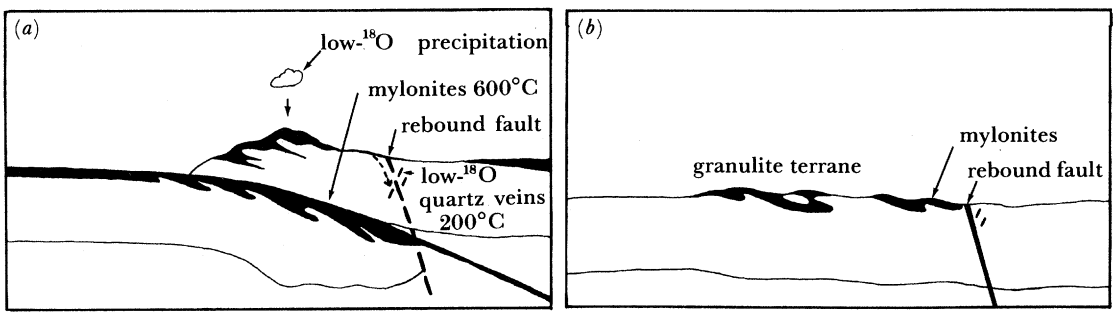

FIGURE 8. Possible tectonic régimes of mylonites and late low-^{18}O quartz veins, Grenville Front. (*a*) Actual collision, subsequent uplift; (*b*) Precambrian crust today.

5. Shear-zone-hosted uranium in overthrust Archaean gneisses, Bahia, Brazil

Uranium deposits in the 10^5 t U_3O_8 range occur within ductile shear zones transecting high-grade Archaean basement gneisses at Lagoa Real in the State of Bahia, Brazil. The mineralization is associated with retrograde metamorphism and extensive sodium metasomatism of host felsic–gneissic basement rocks (Lobato *et al.* 1983*a*). Preliminary oxygen isotope studies

of the uranium deposits together with their host gneisses revealed that the uraninite was precipitated from hydrothermal solutions of meteoric origin ($\delta^{18}O \leqslant -2‰$) at temperatures of 550 °C (Lobato *et al.* 1983*a*, *b*, *c*; figure 9*a*).

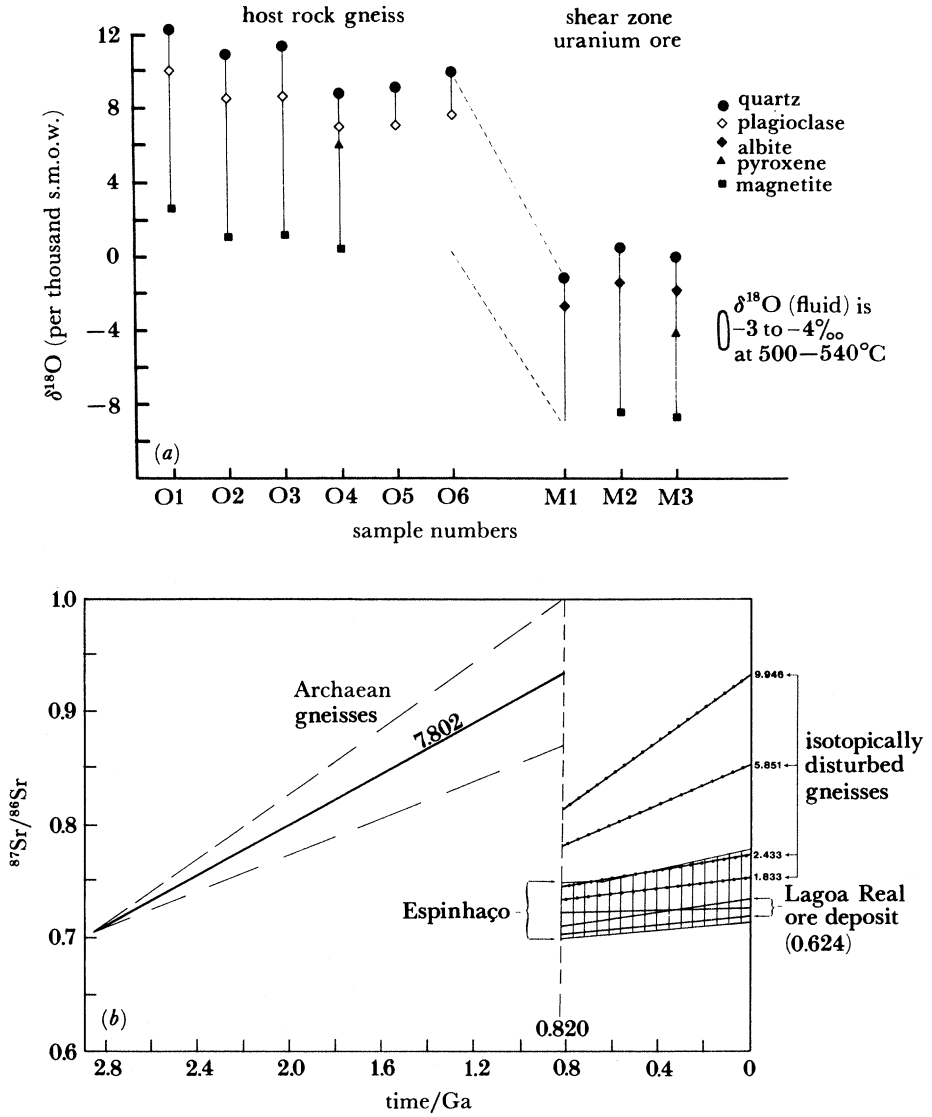

FIGURE 9. (*a*) Values of $\delta^{18}O$ of specified minerals in shear zones and wall rocks, Lagoa Real, Brazil (after Lobato *et al.* 1983*a*). (*b*) $^{87}Sr/^{86}Sr$ of specified rock reservoirs at Lagoa Real, Brazil (after Kerrich *et al.* 1986).

A model in which amphibolite and granulite facies basement gneisses were transported over Proterozoic greenschist facies metasediments of the Espinhaco sequence along a thrust surface has been proposed by Lobato *et al.* 1983*a*, *b*, *c*. Such a mechanism, involving tectonic emplacement of portions of hot basement over colder, wet rocks, would induce dehydration and overpressure meteoric water charged aquifers, causing the high fluid pressures necessary to maintain thrust motion (cf. Fyfe *et al.* 1978).

Calculated or measured $\delta^{18}O$ and δD values of hydrothermal solutions implicated in the mineralization can provide information on the original fluid reservoir. However, identifying

the rock reservoir(s) that donated metals to any specified deposit is a more subtle and less tractable problem. The question of uranium provenance for the shear-zone-hosted uraninite deposits has been addressed by using Rb/Sr isotopic tracer studies. Co-enrichment in Sr and U during hydrothermal alteration can be deduced on the basis of mineralogical and textural relations, and chemical mass balance in the ore deposits. However, this does not necessarily imply that uranium and strontium have been leached from a common rock reservoir. Despite this, strontium isotope tracer studies can constrain the possible rock reservoirs with which the hydrothermal solutions equilibrated.

The Na metasomatic alteration extends over a band about 40 km wide and 100 km long, parallel to the regional strike. Along this band, regional Archaean quartz-microcline–biotite–hornblende gneisses have been transformed to albitites preferentially within shear zones that are collinear with the regional foliation. Uranium enrichment is confined to the albitites. Uraninite forms round crystals associated with mafic minerals, and with albite.

In summary, the shear-zone-related alteration includes (i) replacement of microcline by albite; (ii) dissolution of quartz; (iii) formation of pyroxene and garnet; (iv) oxidation of magnetite to haematite; and (v) epidote forming after pyroxene at later stages of mineralization. Thorough descriptions of all rock types, their geochemistry and mineralogy can be found in Lobato (1983*c*).

Shear-zone-hosted uranium deposits at Lagoa Real, are particularly suited to strontium isotope tracer studies. Four possible strontium donor reservoirs can be envisaged: Archaean gneisses, Proterozoic rocks, sea water and alkaline intrusive rocks. The Archaean gneisses have a Rb/Sr isochron age of 2.86 Ga (U. G. de Cordani 1982, unpublished results), elevated Rb/Sr, and therefore have evolved along a steep $^{87}Sr/^{86}Sr$ trajectory through time. The Espinhaco sequence is substantially younger, with a Rb/Sr isochron age of 1.0 Ga for volcanic rocks of the Boquira Formation. Hydrothermal alteration of deformed gneisses accompanying uraninite deposition resulted in almost total loss of Rb, with concomitant gains of Sr (Lobato *et al.* 1983*b*). Thus Rb/Sr ratios in the deposit and its altered host rock are less than 0.01, such that little ^{87}Sr has been evolved.

Establishing the source of strontium in the uranium deposit requires a knowledge of the mean $^{87}Sr/^{86}Sr$ ratio of each of the possible donor reservoirs at the time of uranium introduction. The best current estimate of the age of uranium mineralization is 820 Ma, by $^{207}Pb/^{206}Pb$ age determination (Stein 1980). An average value for the $^{87}Sr/^{86}Sr$ ratio of the gneisses at 820 Ma can be estimated from isochron data (de Cordani 1982). Taking the average $^{87}Rb/^{86}Sr$ ratio (7.8), the initial $^{87}Sr/^{86}Sr$ ratio at the time of last strontium isotope homogenization (0.705 at 2.86 Ga), and the elapsed time to mineralization, a mean $^{87}Sr/^{86}Sr$ ratio of 0.935 at 820 Ma is obtained. This assumes that the samples used to construct the isochron are representative of the gneisses as a whole. An array for the strontium isotope evolution of the gneisses is portrayed in figure 9*b*, calculated from the mean $^{87}Rb/^{86}Sr$ and $Rb/Sr \pm 2$ of the mean (Kerrich *et al.* 1985).

A second approach to estimating the $^{87}Sr/^{86}Sr$ of the gneisses at 820 Ma uses a suite of samples collected from the vicinity of ore bodies, but external to the shear zones. Back extrapolation of analytically determined $^{87}Sr/^{86}Sr$ ratios, by using measured $^{87}Rb/^{86}Sr$, gives a mean of 0.770 at 820 Ma. This second estimate is significantly lower than that calculated from the isochron data, and is interpreted to reflect lowering of the $^{87}Sr/^{86}Sr$ ratio of the gneisses by infiltration of hydrothermal fluids with a relatively low $^{87}Sr/^{86}Sr$ ratio, during uranium mineralization (see Kerrich *et al.* 1985).

PHILOSOPHICAL TRANSACTIONS OF THE ROYAL SOCIETY A MATHEMATICAL, PHYSICAL & ENGINEERING SCIENCES

At 820 Ma, the Proterozoic Espinhaco had a calculated range in $^{87}Sr/^{86}Sr$ of 0.700–0.740, and a mean of 0.732. Though slightly higher, this ratio is close to that of the uranium deposit (figure 9*b*). Contemporaneous marine water was 0.708 (Veizer & Compston 1974). Measured $^{87}Sr/^{86}Sr$ ratios of the ore deposit are uniform, in keeping with their low Rb/Sr ratios. The deposit is projected to have been characterized by $^{87}Sr/^{86}Sr = 0.719$ at 820 Ma. Strontium evolution arrays are depicted for all of the rock reservoirs considered in figure 9*b*. From these data is it clear that at 820 Ma the Proterozoic Espinhaco had an $^{87}Sr/^{86}Sr$ ratio close to that of the uranium deposit.

As described above, volcanic rocks of the lower Espinhaco formed at 1.1 Ga. If fluid recharge of aquifers in the Espinhaco was from continental meteoric waters as indicated by the $^{18}O/^{16}O$ results, then their strontium isotopic signature would reflect mixing between strontium indigenous to the recharge water and that donated by the Espinhaco metasediments.

Other possible rock reservoirs cannot be ruled out as strontium donors, and mixtures of strontium from sea water and the gneisses remains an alternative explanation. However, taken in conjunction with constraints imposed by field relations, mineralogy and $^{18}O/^{16}O$ data, it is concluded that strontium in the ore body was originally indigenous to the Proterozoic Espinhaco, having been transported to the site of deposition by high-temperature hydrothermal fluids originating as formation brines in the Espinhaco and discharged through shear zones in response to the thrust mechanism as discussed by Lobato *et al.* (1983*a*, *c*).

6. Metamorphic core complex detachment faults

Metamorphic core complexes constitute a unique structural entity in the tectonic architecture of the North American Cordillera. They are broadly domal physiographic features, characterized geologically by a basal core of intensely deformed metamorphic or plutonic rocks, grading upwards through mylonitic equivalents to low-angle planar breccia zones delimiting a detachment fault. This 'infrastructure', or lower plate, is overlain by a 'suprastructure', or upper plate, composed of listrically faulted, allochthonous and generally unmetamorphosed Tertiary rocks (for an overview see Coney (1980)). Twenty-five such core complexes have been identified to date, discontinuously arrayed along the axis of the North American Cordillera (Coney 1980).

Chloritic breccias (characterized by pervasive transgranular fracturing, propylitic alteration and hydraulic fractures occupied by veins) superimposed on the mylonitic rocks are a prominent feature of metamorphic core complexes. Breccia zones are coplanar with detachment faults, which are also the sites for local Cu/Au mineralization, with associated haematite and Mn oxide-bearing vein networks. These features raise questions about the nature of fluid régimes responsible for metasomatic alteration and fracturing along the plane of detachment.

Following the 'landmark' papers of Smoluchowski (1909) and Hubbert & Rubey (1959) on the mechanics of overthrust faulting, it has been an axiom of tectonics that anomalous fluid pressures reduce normal stress by an amount equal to P_{fluid}, thereby diminishing the frictional sliding resistance at thrust surfaces. Recognition of anomalously high fluid pressures as a critical parameter in rock mechanics has raised questions on the source, volume, evolution and thermal régime of fluid reservoirs involved in crustal-scale thrust motion (Fyfe & Kerrich 1983, 1985; Kerrich *et al.* 1984). Whereas some thrust faults are not notably metasomatized, other examples, including those of the Arizona metamorphic core complexes, are characterized by extensive hydrothermal mineralization in contiguous rocks (Coney 1980; Crittendon *et al.* 1980). With

PHILOSOPHICAL TRANSACTIONS OF THE ROYAL SOCIETY A MATHEMATICAL, PHYSICAL & ENGINEERING SCIENCES

these considerations in mind this section reports oxygen isotope data that reveal the nature of large-scale fluid régimes accompanying thrust faulting in detachment zones of southern Arizona (see Kerrich & Rehrig 1986).

The Picacho Mountains are located near Phoenix in S Arizona, and constitute the southerly extension of the array of metamorphic core complexes aligned along the North American Cordillera (Crittendon *et al.* 1980). Geological descriptions of the area are given by several authors, most recently by W. A. Rehrig & S. B. Keith (1984, unpublished results). Geological relations of the Picacho area resemble those of a typical metamorphic core complex (cf. Crittendon *et al.* 1980). The key geological components are three tectonic plates, or thrust blocks, separated by two intervening detachment thrusts. Undeformed to mylonitic granite of the lower plate is demarked by a lower detachment thrust and underlain by chloritic breccia. Variably altered and fractured granitic rocks of the middle plate are bounded by an upper detachment zone upon which allochthonous volcanic and sedimentary rocks of Miocene age lie (figure 10*b*).

Rocks of the lower plate are hornblende–biotite granitic basement (*ca.* 1.4 Ga), locally termed the Oracle granite. Towards the lower detachment thrust a transition occurs from undeformed granitic precursor to progressively more mylonitic products. Mylonites are characterized by ductile flow involving intracrystalline grain-size reduction along with a stretching lineation. This same gradient of deformation, occurring in a 24 Ma granodiorite pluton that intrudes the Oracle granite, establishes the mylonitization as mid Tertiary in age.

Immediately below the lower detachment thrust, mylonites give way to a domain of intense transgranular fracturing: this is accompanied by the reaction of biotite to chlorite, and of oligoclase to albite, producing the 'so-called' chlorite breccias. Middle-plate rocks are composed of 30–40 m thickness of granitic rocks, probably also of Oracle protolith. The salient features are extensive brecciation with concomitant fracture-related hydrothermal alteration dominated by the propylitic mineral assemblage chlorite, epidote, quartz, albite, pyrite, $\pm$carbonate, $\pm$haematite. This is the characteristic mineral assemblage of chloritic breccias, typical of core-complex detachment zones (Phillips 1980).

Dacite–rhyodacite volcanics and sedimentary rocks of Miocene age constitute the upper-plate allochthon. The volcanics have experienced intensive low-temperature oxidative alteration such that the dominant secondary minerals are K feldspar, calcite, haematite and manganese oxides. Lake and hydrothermal travertine–barite deposits are present at the scarps of listric normal faults in the upper plate (figure 10*b*).

At the Picacho tectonic section the salient isotopic features are an upwards trend of whole-rock ^{18}O values from 7.6 to 18.9, in conjunction with a decrease of estimated ambient temperature from 550 to 150 °C. (figures 10*b*, 11). In undeformed Oracle granite of the lower-plate quartz ($\delta^{18}O = 9.1$–10.8), feldspar (7.5–8.2‰) and hornblende (4.9–5.6‰) possess near-magmatic isotopic fractionations. Calculated isotopic temperatures of 500–600 °C are comparable to those deduced for slowly cooled plutonic felsic batholiths. The persistence of high-temperature amphibole is consistent with retention of a near-magmatic isotopic signature. The whole-rock $\delta^{18}O$ value of 7.6 places the Oracle granite in the normal ^{18}O class of plutonic granitic rocks of Taylor (1978) ($6 < \delta^{18}O < 10$). A calculated $\delta^{18}O$ value of 7 for H_2O in equilibrium with feldspars is appropriate for magmatic fluids of normal ^{18}O granites (figure 11).

Mylonitic counterparts of the Oracle granite within the lower plate have a small but systematic ^{18}O shift in quartz relative to their undeformed precursors: accordingly, the

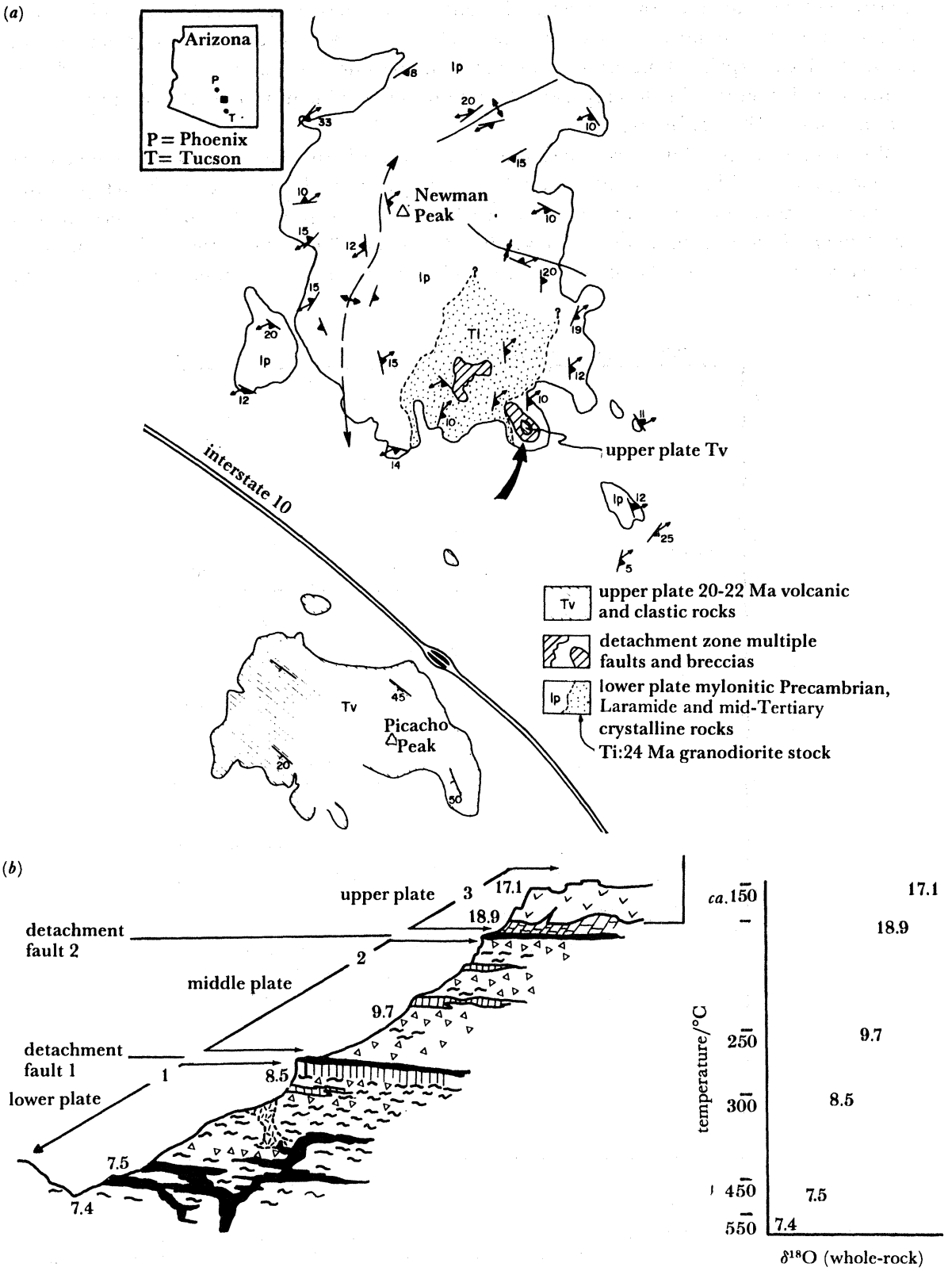

FIGURE 10. (*a*) Schematic geological map of the Picacho metamorphic core complex, Arizona. (*b*) Tectonic cross section with measured $\delta^{18}O$ (whole-rock) values (after Kerrich & Rehrig 1986).

PHILOSOPHICAL TRANSACTIONS OF THE ROYAL SOCIETY A MATHEMATICAL, PHYSICAL & ENGINEERING SCIENCES

quartz–feldspar fractionations are larger. Fractionations amongst quartz, feldspar, biotite and magnetite signify temperatures of 350–500 °C – these are regarded as a dynamic and metamorphic overprint of the granitic protolith, and pertain to the ambient thermal conditions of mylonite formation. Such temperature estimates are commensurate with considerations of the thermal stability of biotite.

Whole-rock oxygen isotope compositions of the mylonitic rocks are identical to undeformed Oracle granite, within the limits of analytical uncertainty. Hence the mylonites probably developed under conditions of low water/rock ratio in the presence of fluids derived from breakdown of hydrous minerals in the granitic precursor. The $\delta^{18}O$ values of these fluids are calculated at 3–6‰, and the fluids are probably mainly of metamorphic origin (figures 2*a* and 11).

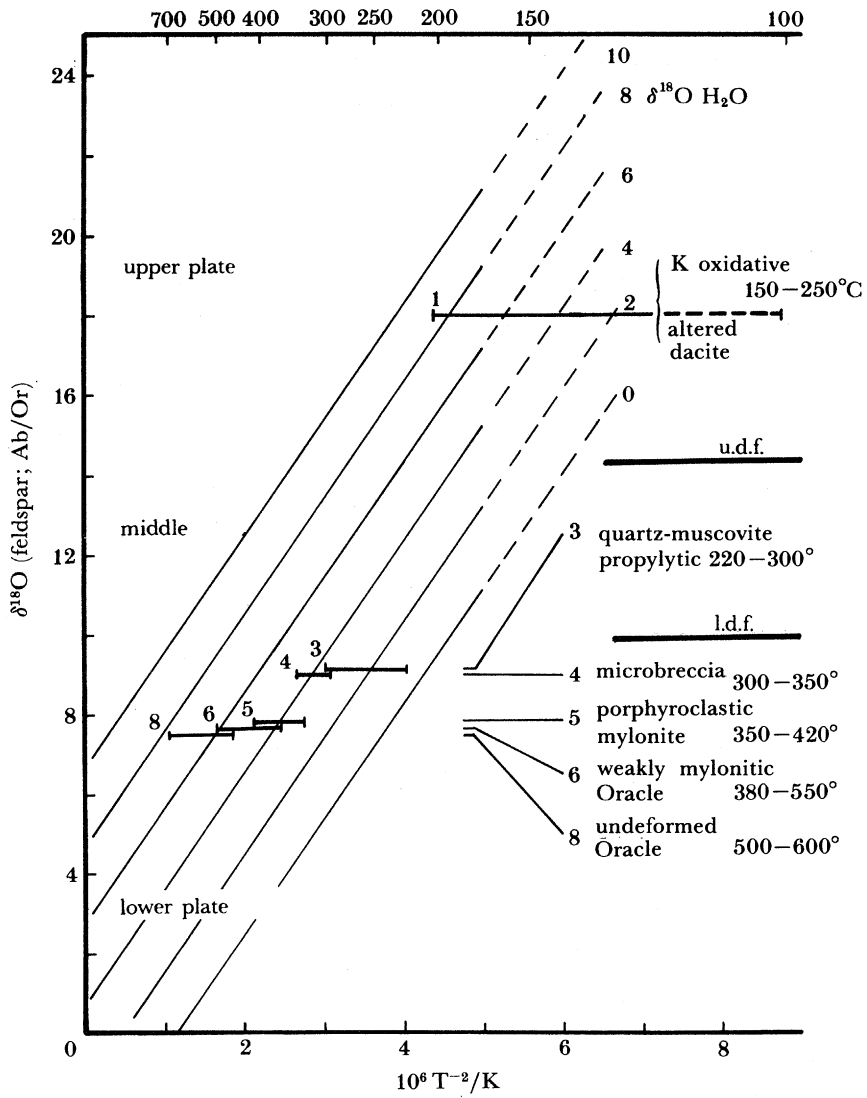

FIGURE 11. Values of $\delta^{18}O$ feldspar plotted against temperature, as estimated on the basis of mineralogical criteria and oxygen isotope fractionations for the Picacho section. The family of lines represent the $\delta^{18}O$ value of water in equilibrium with albite or K feldspar of specified $\delta^{18}O$, at given temperatures. U.d.f., upper detachment fault; l.d.f., lower detachment fault.

Brecciated mylonite, which underlies the lower detachment surface, has $\delta^{18}O$ (quartz) = 11.6, and has thus experienced a positive ^{18}O shift of 2.3‰ relative to quartz in the underlying ductile mylonitic precursors of the breccia. Fractionations amongst quartz, feldspar and chlorite correspond to isotopic temperatures of 300–350 °C. The positive shift in quartz is accompanied by a whole-rock shift of 1‰ compared with mylonitic and pristine Oracle granite: these relations require that the breccia has experienced fluid fluxing to account for the measured isotopic excursion. Lower inferred temperatures for fracturing relative to mylonites are in accord with the transformation of biotite to chlorite, and the evidence for fluid incursion is in harmony with field evidence for multiple vein generation. Hydrothermal fluids in equilibrium with the chlorite breccia have a calculated $\delta^{18}O$ of 4 ± 1. Thus the breccia marks a structural–hydrological domain representing the boundary from a lower zone of low water/rock ratio to an upper zone of high fluid fluxes.

Veined and hydrothermally altered rocks of the middle plate have elevated $\delta^{18}O$ values for quartz (12‰) and whole-rock (9.7‰) relative to the underlying plate, and thus define a progressive trend of ^{18}O enrichment up the structural section. Temperatures of alteration are estimated to be 220–330 °C, in the presence of $\delta^{18}O$ (fluid) = 2–5‰.

Temperatures of hydrothermal alteration in volcanic rocks of the upper plate cannot readily be estimated. Assuming a span of 100–200 °C, fluids of −3 to +8‰ are implicated in the oxidative event that produced K-feldspar, illite, haematite and manganese oxides. Calcite, at 22‰ would have been in equilibrium with fluids of 5‰ at 100 °C. The $\delta^{13}C$ at −0.8 to −2.9 is not alone diagnostic of the source of carbon in altered volcanics of the upper plate.

In summary, upwards in the tectonic section, temperatures progressively diminish, whole-rock ^{18}O values increase dramatically, and calculated fluid $\delta^{18}O$ values generally fall in a narrow range of 3–7‰. These relations are interpreted to signify expulsion of metamorphic fluids from mylonites of lower structural levels, through the middle and into rocks of the upper plate, accompanied by cooling. Sporadic fracture-related ^{18}O-depleted albite and K feldspar (2–11‰) implicates incursion of low-^{18}O meteoric thermal waters into the upper plate, along listric normal faults. Thus the tectonic section records an upwards transition from high to low ambient temperature, low to elevated water/rock ratio, ductile to brittle deformation, and a fluctuating interface of deep metamorphic with shallow surface aqueous reservoirs.

7. Summary and conclusions

(*a*) *Archaean fault systems*

The principal conclusions on the nature of fluid transport in structural lineaments of the Abitibi Greenstone Belt are as follows.

(1) Major linear structures were probably initiated as listric normal faults, accommodating extension of the greenstone belt, and acting as sites for the extrusion of komatiitic magmas. They also formed submarine scarps which delimit linear belts of submarine clastic to volcaniclastic sediments. At this stage of greenstone belt development intense marine-water hydrothermal activity proceeded both in and peripheral to fault zones, locally generating linear belts of chemical sedimentary rocks such as iron formation.

(2) Subsequently, reverse motion occurred on the structures, accommodating shortening of a greenstone belt under compression. At this stage, fault zones acted as conduits for the ascent of trondhjemitic and alkaline magmas, as well as for the discharge of hydrothermal fluids.

PHILOSOPHICAL TRANSACTIONS OF THE ROYAL SOCIETY A MATHEMATICAL, PHYSICAL & ENGINEERING SCIENCES

(3) The hydrothermal fluids were probably of metamorphic origin, derived by devolatilization of crust undergoing thermal prograding: a magmatic fluid contribution is possible.

(4) Fluids carried more radiogenic Sr and Pb than contemporaneous mantle or mafic volcanic crust, and were thus derived from devolatilization of sialic basement in addition to the supracrustal sequence.

(5) Mineralized structures are characteristically enriched in certain large-ion lithophile elements including K, Rb, Li, Cs and B (etc.) as well as rare elements such as Au, Ag, As, Sb, Se, Te, Bi, Pb and W. Structures act therefore as sites for geochemical transfer between lower and upper lithosphere.

(6) Fluids were characterized by $X_{CO_2} \approx 0.1$, neutral to slightly acidic pH, low salinity (less than 3% by mass) K/Na = 0.1, carried minor CH_4, CO and N_2, and underwent transient effervescence of CO_2 during decompression.

(*b*) *General discussion*

In general, fluid régimes in the fault and shear zones studied follow a sequence from conditions of high temperature and pressure with locally derived fluids at low water/rock ratios, during initiation of the structures, to high fluid fluxes along discrete conduits as the structures propagate, develop large-scale permeability and penetrate hydrothermal reservoirs. At this second stage, discharging fluids were at high temperature and pressure and reduced, because of their transport upwards from deeper crustal levels: such fluids were predominantly of metamorphic origin, their characteristic high $\delta^{18}O$ values reflecting equilibrium of the reservoir with crustal rocks at elevated temperatures in the source region.

Later in the tectonic evolution, as deeper crustal levels were exposed by erosion such that conditions of lower ambient temperature and pressure prevailed, incursion of near-surface waters into faults occurred: these fluids were either formation brines in aquifers intersected by the fault or from direct downwards penetration of surface fluids into the structures. Such fluids were oxidized and of lower $\delta^{18}O$ value, the former reflecting near-surface environments, and the latter commensurate with a component of low-^{18}O meteoric continental surface water, or shallower level metamorphic fluids where the $\delta^{18}O$ is buffered to smaller values by larger rock/water fractionations at the lower ambient temperatures. The high-temperature–high-^{18}O, and low-temperature fluid régimes of faults may proceed coevally, the former at deep and the latter at shallow crustal levels, with juxtaposition of the two taking place by subsequent vertical displacements on the structure. Flow of both deep-level (metamorphic) and shallow-level (meteoric) fluids has been implicated in contemporary seismic activity on the San Andreas fault by Irwin & Barnes (1975) and Sibson (1981*a*, *b*, 1982) respectively.

At higher crustal levels, significant infiltration of meteoric water along major thrust faults has been identified. Lee *et al.* (1984) have shown that the δD, $\delta^{18}O$ and apparent K/Ar ages of Mesozoic and Tertiary plutons in Nevada have been disturbed in proximity to the Snake Range décollement. In Oligocene plutons (37 Ma) deformed cataclastically, $\delta^{18}O$, δD and K/Ar ages are as low as $-2.5‰$, $-155‰$, and 18 Ma respectively, because of deformation combined with incursion of isotopically light thermal waters. For undeformed Jurassic plutons, $\delta^{18}O$ values are undisturbed, but both δD values and K/Ar ages have been perturbed over distances of tens of metres below the décollement.

The Bitterroot Lobe–Sapphire Block detachment zone of western Montana is defined by a 500 m thick sequence of mylonitic granites, locally overprinted by chloritic breccias

characterized by intense transgranular fracturing. Kerrich & Hyndman (1985) have shown that the ductile mylonites formed at 550 ± 50 °C, in the presence of magmatic, or high-temperature metamorphic fluids. Chloritic breccias are depleted in ^{18}O by about 10‰ relative to mylonitic precursors, and appear to have formed under conditions of lower temperature (250–370 °C) and lower effective confining stress, acting as an aquifer for the infiltration of low-^{18}O surface meteoric waters ($\delta^{18}O$ values of -7 to -12‰).

At Lagoa Real, discharge of the low-^{18}O fluids of surface-water origin probably took place at *ca.* 15 km depth in the crust and at relatively high temperatures of 550 °C. This situation appears to have taken place during overriding of a sedimentary sequence with meteoric water recharged aquifers, by high-grade gneisses during overthrusting.

The role of metamorphic fluids in shear zones at deep crustal levels has been emphasized by Beach & Fyfe (1972), Beach (1976) and Kerrich & Fyfe (1981). Etheridge *et al.* (1984) present evidence for high pore fluid pressures during prograde regional metamorphism, with resultant low effective confining stress, leading to enhanced permeabilities, and in turn to the local dominance of advective flow. All of these studies, including the present one, emphasize that large-scale fluid flow may occur at deep crustal levels under appropriate conditions. On the other hand, some shear zones appear to have been essentially chemically and hydrologically closed systems. This is so for the Mieville Shear Zone transecting Hercynian granodiorite of the Aiguilles Ranges, Switzerland, where no significant excursions of $\delta^{18}O$ (rock) values, oxidation state, or rock composition occur from the protolith across the structure (Kerrich *et al.* 1980).

In addition to the mechanical effects of transient high fluid pressures in faults (Kerrich & Allison 1978; Sibson 1981 *a*, *b*) modification of ambient chemical conditions by fluids streaming through faults may play a role in silicate deformation. As discussed above, the oxidation state of iron in some structures indicates significant reduction by fluids, probably owing to elevated partial pressures of hydrogen, and it is possible that such high P_{H_2} may influence the cracking behaviour of minerals in the fault zone. For instance, hydrogen embrittlement is a well known phenomenon in metals and ceramics, and is thought to occur by chemisorption of hydrogen at fracture surfaces, which promotes nucleation of dislocations at crack tips (Lynch 1979; Michalske & Freiman 1982). Hobbs (1983) notes that at an intracrystalline level, incorporation of a hydrogen defect that is capable of acting as an acceptor into silicates leads to a strong dependence of point-defect chemistry on the fugacities of both water and oxygen.

Strontium isotope data have been used in a number of studies of hydrothermal systems to address the solute-source problem. Taylor & Fryer (1983) described variable degrees of enrichment in ^{87}Sr of hydrothermally altered domains within the Santa Rita porphyry copper deposit, attributed to the addition of Sr from Palaeozoic–Mesozoic carbonate host rocks ($^{87}Sr/^{86}Sr = 0.7084$–0.7088) via an external aqueous reservoir to the stock ($^{87}Sr/^{86}Sr = 0.7057$–0.7058). The Pasto Bueno tungsten and base-metal sulphide deposit, Peru, is associated with a 10 Ma quartz monzonite stock ($^{87}Sr/^{86}Sr = 0.7056$–0.7074), which intruded a Jurassic shale (0.7169) and Cretaceous quartzite (0.7158). Norman & Landis (1983) determined that the $^{87}Sr/^{86}Sr$ of gangue minerals and fluid inclusion water ranged from 0.7058–0.7239, with $Rb/Sr < 0.027$. The lowest ratios correspond to magmatic fluids from the host Tertiary intrusion, and more radiogenic values to Sr leached from the host sediments or Palaeozoic–Precambrian basement. Two critical points were demonstrated by Norman & Landis (1983): first that measured variations in mineralization do not correlate with the $^{87}Sr/^{86}Sr$ of wall rocks, and second, that systematic variations between $^{87}Sr/^{86}Sr$ and stable

isotope compositions of fluids rule out the likelihood that the most radiogenic values are a result of selective leaching of Rb-rich phases.

During hydrothermal alteration of ocean-floor rocks in the presence of sea water, the $^{87}Sr/^{86}Sr$ ratio of tholeiites (*ca.* 0.703) is shifted off the primary Sr/Nd isotope mantle array, in the direction of higher Nd towards the limiting value of contemporaneous sea water (0.709) (Spooner *et al.* 1977; O'Nions *et al.* 1979). Formation brines within the Canadian Shield possess $^{87}Sr/^{86}Sr = 0.711–0.740$, generally reflecting equilibrium with the contemporary local rock Sr isotope ratio (table 1 of McNutt *et al.* 1984). Shear zones in the Willamaya Complex, Broken Hill, Australia, plot above the 1665 Ma isochron of the Potosi gneiss host. Etheridge & Cooper (1981) attribute introduction of the radiogenic Sr, coupled with SiO_2-, K_2O- and Ba-leaching, to large-scale fluid flow through the shear zone where fluids ($^{87}Sr/^{86}Sr = 0.794$) had interacted with the Willamaya Complex metamorphics.

These, along with many other studies, demonstrate that where geological boundary conditions are appropriate, combined light stable isotope and Sr isotope tracer studies may resolve the question of fluid and solute source reservoirs for domains of hydrothermal metasomatism.

References

Almeida, F. F. M. 1977 *Rev. Bras. Geoscienc.* **7**, 349–364.

Barker, R. F. 1979 Trondhjemites: definition, environment and hypotheses of origin. In *Trondhjemites, dacites, and related rocks, developments in petrology*, vol. 6 (ed. F. Barker). Amsterdam: Elsevier.

Barker, F., Arth, J. G. & Millard, H. T. 1979 Trondhjemite: definition, environment and hypotheses of origin. In *Trondhjemites, dacites, and related rocks, developments in petrology*, vol. 6 (ed. F. Barker). Amsterdam: Elsevier.

Barker, F., Arth, J. G. & Millard, H. T. 1979 Archean trondhjemites of the Southwestern Big Horn Mountains, Wyoming: a preliminary report. In *Trondhjemites, dacites and related rocks, developments in petrology*, vol. 6 (ed. F. Barker), pp. 401–414. Amsterdam: Elsevier.

Beach, A. & Fyfe, W. S. 1972 Fluid transport and shear zones at Scourie, Sutherland: evidence for overthrusting? *Contrib. Miner. Petrol.* **36**, 75–180.

Beach, A. 1976 The interrelations of fluid transport, deformation, geochemistry and heat flow in early Proterozoic shear zones in the Lewisian complex. *Phil. Trans. R. Soc. Lond.* A **280**, 569–604.

Boyle, R. W. 1961 The geology, geochemistry, and origin of the gold deposits of the Yellowknife district. *Mem. geol. Surv. Can.* **310**, 193.

Boyle, R. W. 1979 The geochemistry of gold and its deposits. *Bull. geol. Surv. Can.* **280**, 548.

Breakey, A. R. 1975 *A mineralogical study of the gold quartz lenses in the Campbell shear, Con Mine, Yellowknife, N.W.T.* M.Sc. thesis, McGill University, Montreal.

Colvine, A. C. 1984 An integrated model for the origin of Archean gold deposits. *Ontario Geological Survey, Open File Rep. 5524.* (98 pages.)

Coney, P. J. 1980 Cordilleran metamorphic core complexes: An overview. *Mem. geol. Soc. Am.* **153**, 7–34.

Collerson, K. D. & Fryer, B. J. 1978 Role of fluids in the formation and subsequent development of early continental crust. *Contrib. Miner. Petrol.* **67**.

Crittenden, M. D., Jr, Coney, P. J. & Davis, G. H. 1980 Cordilleran Metamorphic Core Complexes. *Mem. geol. Soc. Am.* **153**.

Etheridge, M. A. & Cooper, J. A. 1981 Rb/Sr isotopic and geochemical evolution of a recrystallized shear (mylonite) zone at Broken Hill. *Contrib. Miner. Petrol.* **78**, 74–84.

Etheridge, M. A., Cox, S. F., Wall, V. J. & Vernon, R. H. 1984 High fluid pressures during regional metamorphism and deformation: implications for mass transport and deformation mechanisms. *J. geophys. Res.* **89**, 4344–4358.

Eugster, H. P. & Skippen, G. B. 1967 Igneous and metamorphic reactions involving gas equilibria. In *Researches in geochemistry*, vol. 2 (ed. P. H. Abelson), pp. 492–520. New York: John Wiley.

Faure, G. 1977 *Principles of isotope geology.* (464 pages.) Toronto: John Wiley & Sons.

Foy, R. 1985 Geology of Kirkland and Larder Lakes, northern Ontario. B.Sc. thesis, University of Western Ontario.

Franklin, J. M., Roscoe, S. M., Loveridge, W. D. & Sangster, D. F. 1983 Lead isotope studies in Superior and Southern provinces. *Bull. geol. Surv. Can.* **351**, 60.

Friedman, I. & O'Neil, J. R. 1977 Compilation of stable isotope fractionation factors of geochemical interest, In *Data of geochemistry, U.S.G.S. prof. paper 440.*

PHILOSOPHICAL TRANSACTIONS OF THE ROYAL SOCIETY A MATHEMATICAL, PHYSICAL & ENGINEERING SCIENCES

Fryer, B. J., Kerrich, R., Hutchinson, R. W., Peirce, M. G. & Rogers, D. S. 1979 Archean precious metal hydrothermal systems, Dome Mine, Abitibi greenstone belt, I. *Can. J. earth Sci.* **16**, 421–439.

Fyfe, W. W. & Henley, R. W. 1973 Some thoughts on chemical transport processes with particular reference to gold. *Minerals Sci. Engng* **5**, 295–303.

Fyfe, W. S. & Kerrich, R. 1983 Fluid release and mineralization associated with thrusting. *Fourth International Symposium on water–rock interaction, Misasa, Japan*, pp. 150–151. Int. Assoc. of Geochem. Cosmochem.

Fyfe, W. S. & Kerrich, R. 1985 Fluids and thrusting. *Chem. Geol.* **49**, 353–362.

Fyfe, W. S., Price, N. J. & Thompson, A. B. 1978 *Fluids in the Earth's crust*. Amsterdam: Elsevier.

Fyon, J. A., Crocket, J. H. & Schwarcz, H. P. 1983 Application of stable isotope studies to gold metallurgy in the Timmins–Porcupine camp. Ontario Geoscience Research Grant Program, grant 49, *O.G.S. Open File Rep.* 5464. (182 pages.)

Fyon, J. A., Schwarcz, H. P., Crocket, J. H. & Knyf, M. 1982 Gold exploration potential using oxygen, carbon, and hydrogen stable isotope systematics of carbonatized rocks and quartz veins, Timmins area. In *Ont. Geol. Surv. misc. pap. 103* (ed. E. G. Pye), pp. 59–64.

Fyon, J. A., Schwarcz, H. P. & Crocket, J. H. 1984 Carbonization and gold mineralization in the Timmins area, Abitibi greenstone belt: genetic links with Archean mantle CO_2-degassing and lower crust granulitization. *Geol. Ass. Can. Prog. Abstr.* **9**, 65.

Gates, T. M. & Hurley, P. M. 1973 Evaluation of Rb/Sr dating methods applied to Matachewan, Abitibi, Mackenzie, and Sudbury dike swarms in Canada. *Can. J. earth Sci.* **10**, 900–919.

Geisel Sobrinho, E., Raposo, C., Alves, J. V., de Brito, W. & Vasconcelos, J. G. 1980 O distrito uranifero de Laqoa Real, Bahia. *Anais XXXI Congr.*

Golding, S. D. & Wilson, A. F. 1983 Geochemical and stable isotope studies of the no. 4 lode, Kalgoorlie, Western Australia. *Econ. Geol.* **78**, 438–450.

Goodwin, A. M. & Ridler, R. H. 1970 The Abitibi orogenic belt. *Can. Geol. Surv. pap. 70–40*, pp. 1–31.

Harrison, I. M. 1983 Some observations on the interpretation of $^{40}Ar/^{39}Ar$ age spectra. *Isotope Geosci.* **1**, 319–338.

Hart, S. R. & Brooks, C. 1974 Clinopyroxene–matrix partitioning of K, Rb, Cs, Sr, and Ba. *Geochim. cosmochim. Acta* **38**, 1799.

Helgeson, H. C. & Garrels, R. M. 1968 Hydrothermal transport and deposition of gold. *Econ. Geol.* **63**, 622–635.

Henderson, J. F. & Brown, I. C. 1966 Geology and structure of the Yellowknife Greenstone Belt, District of Mackenzie. *Geol. Surv. Can. Bull.* **141**.

Hobbs, B. E. 1984 Point defect chemistry of minerals under a hydrothermal environment. *J. geophys. Res.* **89**, 4026–4038.

Holland, H. D. & Malinin, S. D. 1979 Solubility and occurrence of non-ore minerals. In *Geochemistry of hydrothermal ore deposits* (ed. H. L. Barnes), pp. 461–508.

Hubbert, M. K. & Rubey, W. W. 1959 *Bull. geol. Soc. Am.* **70**, 115–166.

Inda, H. A. V. & Barbosa, J. F. 1978 *Secretaria das Minas e Energia, Estadode Bahia, Salvador.*

Irwin, W. P. & Barnes, I. 1975 Effects of geologic structure and metamorphic fluids on seismic behaviour of the San Andreas fault system in central and northern California. *Geology* **4**, 713–716.

Javoy, M. 1977 Stable isotopes and geothermometry. *J. geol. Soc. Lond.* **133**, 609–636.

Jolly, W. T. 1978 Metamorphic history of the Archean Abitibi belt. *Can. geol. Surv. pap. 78–10*, pp. 367.

Kennedy, L. P. 1985 *The geology and geochemistry of the Archean Flavrian pluton, Noranda, Quebec.* Ph.D. thesis, University of Western Ontario, London, Canada. (469 pages.)

Kerrich, R., Fyfe, W. S. & Allison, I. 1977*a* Iron reduction around gold-quartz veins, Yellowknife district, Northwest Territories, Canada. *Econ. Geol.* **72**, 657–663.

Kerrich, R., Fyfe, W. S., Gorman, B. E. & Allison, I. 1977*b* *Contrib. Miner. Petrol.* **65**, 183–190.

Jensen, L. 1980 Gold mineralization in Kirkland Lake and Larder Lake areas. In *Genesis of Archaean, volcanic-hosted ore deposits* (ed. E. G. Pye & R. G. Roberts), pp. 51–65. Ont. Geol. Surv. Misc. Pap. 97.

Kerrich, R. & Allison, I. 1978 Vein geometry and hydrostatics during Yellowknife mineralization. *Can. J. earth Sci.* **15**, 1653–1660.

Kerrich, R. & Fryer, B. J. 1979 Archean precious metal hydrothermal systems: Dome Mine, Abitibi greenstone belt; II r.e.e. and oxygen isotope relations. *Can. J. earth Sci.* **16**, 440–458.

Kerrich, R., Allison, I., Barnett, R. S., Moss, S. & Starkey, J. 1980 Microstructural and chemical transformations accompanying deformation of granite in a shear zone at Mieville, Switzerland; with implications for stress corrosion cracking and superplastic flow. *Contrib. Miner. Petrol.* **73**, 221–242.

Kerrich, R. & Fyfe, W. S. 1981 The gold–carbonate association: source of CO_2, and CO_2 fixation reaction in Archaean Lode Deposits. *Chem. Geol.* **33**, 265–294.

Kerrich, R. & Hodder, R. W. 1982 Archean lode gold and base metal deposits: chemical evidence for metal separation into independent hydrothermal systems. In *C.I.M. special vol. 24, Geology of Canadian Gold Deposits* (ed. R. W. Hodder & W. Petruk), pp. 144–160. Montreal.

Kerrich, R. 1983 Geochemistry of gold deposits in the Abitibi greenstone belt. *C.I.M. special Pap. 27.*

Kerrich, R., Kishida, A. & Willmore, L. M. 1984 *Geol. Ass. Can. Prog. Abstr.* **9**, 78.

PHILOSOPHICAL TRANSACTIONS OF THE ROYAL SOCIETY A MATHEMATICAL, PHYSICAL & ENGINEERING SCIENCES

Kerrich, R. & Watson, G. P. 1984 The Macassa Mine Archean lode gold deposits, Kirkland Lake, Ontario: geology, patterns of alteration, and hydrothermal régimes. *Econ. Geol.* **79**, 1104–1130.

Kerrich, R., Lobato, L., Fyfe, W. S. & Willmore, L. M. 1986 Shear zone hosted uranium deposits in overthrust Archean gneisses; Bahia, Brazil: evidence on U provenance from Rb/Sr isotopic data. *Econ. Geol.* (In the press.)

Kerrich, R. & Rehrig, W. 1986 Large-scale fluid motion associated with Tertiary mylonitization and detachment faulting: $^{18}O/^{16}O$ evidence from the Pichacho metamorphic core complex, Arizona. *Geology*. (In the press.)

Kerrich, R. & Hyndman, D. 1985 Thermal and fluid régimes in the Bitterroot Lobe–Sapphire Block detachment zone: evidence from $^{18}O/^{16}O$ and geologic relations. *Bull. geol. Soc. Am.* (In the press.)

King, R. 1983 *The auriferous porphyry zone: Taylor Township, Ontario*. B.Sc. thesis, University of Western Ontario.

King, R. & Kerrich, R. 1986 Fluorapatite fenitization and gold concentration, Taylor township, Ontario. *Can. J. Earth Sci.* (In the press.)

Kishida, A. 1984 *Hydrothermal alteration zoning and gold concentration at the Kerr-Addison Mine, Ontario, Canada. Ph.D. thesis, University of Western Ontario, London, Canada.* (231 *pages.*)

Kishida, A. & Kerrich, R. 1985 Hydrothermal alteration zoning and gold concentration at the Kerr-Addison, Archean lode gold deposit, Kirkland Lake, Ontario. *Econ. Geol.* (In the press.)

Krogh, T. E., Davis, D. W., Nunes, P. D. & Korfu, F. 1982 Archean evolution from precise U/Pb isotopic dating. *Geol. Ass. Can. Prog. Abstr.* **7**, 61.

Kwong, Y. T. J. & Crocket, J. H. 1978 Background and anomalous gold in rocks of an Archaean greenstone assemblage, Kakigi Lake area, Northwestern Ontario. *Econ. Geol.* **73**, 50–63.

LaTour, T. E. 1981*a* Significance of folds and mylonites at the Grenville Front in Ontario. *Bull. geol. Soc. Am.* **92**, 997–1038.

Lee, D. E., Friedman, I. & Gleason, J. D. 1984 Modification of δD values in eastern Nevada granitoid rocks spatially related to thrust faults. *Contrib. Miner. Petrol.* **88**, 288–298.

Lemmlein, C. G. & Klevstov, P. V. 1961 Relations among the principal thermodynamic parameters in part of the system $H_2O + NaCl$. *Geochemistry* **2**, 148–158.

Liou, J. G., Kuniyoshi, S. & Ito, K. 1974 Experimental studies of the phase relations between greenschist and amphibolite in a basaltic system. *Am. J. Sci.* **174**, 613–632.

Lobato, L. M., Forman, J. M. A., Fizikawa, K., Fyfe, W. S. & Kerrich, R. 1983*a* Uranium in overthrust Archean basement, Bahia, Brazil. *Can. Miner.* **21**, 647–654.

Lobato, L. M., Forman, J. M. A., Fyfe, W. S., Kerrich, R. & Barnett, R. L. 1983*c* Uranium enrichment in Archean crustal basement associated with overthrusting. *Nature, Lond.* **303**, 235–237.

Lobato, L. M., Fuzikawa, K., Fyfe, W. S. & Kerrich, R. 1983*b* Uranium enrichment in Archean basement: Logoa Real, Brazil. *Rev. Bras. Geocienc.* **12**, 484–486.

Lynch, S. P. 1979 Mechanisms of hydrogen assisted cracking. *Metals Forum* **2**, 189–200.

Mascarenhas, J. de F. & Silvasa, J. H. 1983 Geological and metallogenic patterns in the Archean and Early Proterozoic of Bahia State, Eastern Brazil. *Rev. Bras. Geocienc.* **12**, 193–214.

McNeil, A. M. & Kerrich, R. 1985 Archean lamprophyric dykes gold mineralization, Matheson, Ontario: the conjunction of LIL-enriched mafic magmas, deep crustal structures and Au concentration. *Can. J. earth Sci.* (In the press.)

McNutt, R. H., Frape, S. K. & Fritz, P. 1984 Strontium isotopic composition of some brines from the Precambrian Shield of Canada. *Isotope Geoscience* **2**, 205–215.

Michalske, T. A. & Freiman, S. W. 1982 A molecular interpretation of stress corrsion in silica. *Nature, Lond.* **295**, 511–512.

Montoya, J. W. & Hemley, J. J. 1975 Activity relations and stabilities in alkali feldspar and mica alteration reactions. *Econ. Geol.* **70**, 577–594.

Moutiuba da Costa, L. A. & Inda, H. A. V. 1982 *Ciencias da Terra* **2**, 43–48.

Norman, D. I. & Landis, G. P. 1983 Source of mineralizing components in hydrothermal ore fluids as evidenced by $^{87}Sr/^{86}Sr$ and stable isotope data from the Pasto Bueno Deposit. *Peru. Econ. Geol.* **78**, 451–465.

Nunes, P. D. & Jensen, L. S. 1980 Geochronology of the Abitibi metavolcanic belt, Kirkland Lake area – progress report. In *Summary of geochronology studies 1977–1979* (ed. E. G. Pye). *Ontario geol. Surv. Misc. pap.* **92**, 40–45.

Nunes, P. D. & Pyke, D. R. 1980 Geochronology of the Abitibi Metavolcanic belt, Timmins–Matachewan Area – progress report. In *Ontario geol. Surv.* misc. pap. 92 (ed. E. G. Pye), pp. 34–39.

Ohmoto, H. & Rye, R. O. 1979 Isotopes of sulphur and carbon. In *Geochemistry of hydrothermal ore deposits* (2nd edn) (ed. H. L. Barnes), pp. 509–562. New York: John Wiley & Sons.

O'Nions, R. K., Carter, S. R., Eversen, N. M. & Hamilton, P. J. 1979 Geochemical and cosmochemical applications of Nd isotope analysis. *A. Rev. Earth planet Sci.* **7**, 11–38.

O'Nions, R. K. & Pankhurst, R. J. 1978 In *Trace elements in igneous petrology, developments in petrology*, vol. 5 (ed. C. J. Allegre & S. R. Hart), pp. 211–236. Amsterdam: Elsevier.

Pedreira, A. J., Kishida, A., Torquato, J. R. & Mascarenhas, J. de F. 1978 *Publicacao Especial 3, SBG/SME, Bahia.* (466 pages.)

Phillips, J. C. 1980 In *Mesozoic–Cenozoic tectonic evolution of the Colorado River region, California, Arizona and Nevada*, pp. 109–116. San Diego: Cordilleran Publications.

PHILOSOPHICAL TRANSACTIONS OF THE ROYAL SOCIETY A MATHEMATICAL, PHYSICAL & ENGINEERING SCIENCES

Phillips, J. C. 1982 Character and origin of cataclasite developed along the low-angle Whipple detachment fault, Whipple Mountains, California. In *Mesozoic–Cenozoic tectonic evolution of the Colorado River region, California, Arizona and Nevada* (Anderson–Hamilton volume) (ed. E. G. Frost & D. L. Martin), pp. 109–116.

Pyke, D. R. 1976 On the relationship of gold mineralization and ultramafic volcanic rocks in the Timmins area, northeastern Ontario. *Bull. Can. Inst. Min. Metall.* **69**, 76–87.

Ramsay, J. G. & Graham, R. H. 1970 Strain variation in shear belts. *Can. J. earth Sci.* **7**, 786–813.

Schwarcz, H. P. & Rees, C. E. 1984 $\delta^{34}S$ in pyrite from gold deposits. In *Geoscience research seminar and open house '84, abstracts, Ontario geol. Surv.*, p. 1.

Seward, T. M. 1979 Modern hydrothermal systems in New Zealand and their relation to gold mineralizing processes. *Publ Geol. Dept. Exten.-Serv., Univ. West Australia* **3**, 107–162.

Sibson, R. H. 1977 Fault rocks and fault mechanisms. *J. geol. Soc. Lond.* **133**, 191–213.

Sibson, R. H. 1981 Fluid flow accompanying faulting: field evidence and models. In *Earthquake prediction: an international review*; Maurice Ewing Series vol. 4 (ed. D. W. Simpson & P. C. Richards), pp. 593–604. Washington D.C.: American Geophysics Union.

Sibson, R. H. 1982 Fault zone models, heat flow and the depth distribution of earthquakes in the continental crust. *Bull. seism. Soc. Am.* **72**, 151–163.

Smoluchowski, M. S. 1909 *Geol. Mag.* **6**, 204–205.

Spooner, E. T. C., Chapman, H. J. & Smewing, J. D. 1977 Strontium isotopic contamination and oxidation during ocean floor hydrothermal metamorphism of the ophiolitic rocks of the Troodos Massif, Cyprus. *Geochim. cosmochim. Acta* **41**, 873–890.

Stein, J. H., Netto, A. M., Drummond, D. & Angeiras, A. G. 1980 Nota preliminar sobre os processos de albitizacao uranifera de Lagoa Real (Bahia) e sua comparacao com os da URSS e Suecia. *Anais do XXXII Congr. Bras. de Geol., Santa Catarina* **3**, 1758–1775.

Sunwall, M. T. & Pushkar, P. 1979 *Chem. Geol.* **24**, 189–197.

Taylor, H. P. 1968 Oxygen isotope geochemistry of igneous rocks. *Contrib. Miner. Petrol.* **19**, 1–71.

Taylor, H. P. 1974 The application of oxygen and hydrogen isotope studies to problems of hydrothermal alteration and ore deposition. *Econ. Geol.* **69**, 843–883.

Taylor, H. P. 1978 Oxygen and hydrogen isotope studies of plutonic granitic rocks. In *Trace elements in igneous petrology, developments in petrology*, vol. 5 (ed. C. J. Allegre & S. R. Hart), pp. 177–210. Amsterdam: Elsevier.

Taylor, H. P. 1979 Oxygen and hydrogen isotope relations in hydrothermal mineral deposits. In *Geochemistry of hydrothermal ore deposits* (ed. H. L. Barnes), pp. 237–277. New York: John Wiley.

Taylor, R. P. & Fryer, B. J. 1983 Strontium isotope geochemistry of the Santa Rita porphyry copper deposit, New Mexico. *Econ. Geol.* **78**, 170–174.

Tilling, R. I., Gottfried, D. & Rowe, J. J. 1973 Gold abundance in igneous rocks: bearing on gold mineralization. *Econ. Geol.* **68**, 168–186.

Veizer, J. & Compston, W. 1974 $^{87}Sr/^{86}Sr$ composition of sea water during the Phanerozoic. *Geochim. cosmochim. Acta* **38**, 1461–1484.

PHILOSOPHICAL TRANSACTIONS OF THE ROYAL SOCIETY A MATHEMATICAL, PHYSICAL & ENGINEERING SCIENCES